

Applications of Liquid Crystalline Elastomers

C. Ohm, M. Brehmer, and R. Zentel

Abstract This chapter focuses on recent developments in the field of liquid crystalline elastomers (LCEs) that bring these materials closer to the world of real applications, concentrating on their actuation properties. First, we briefly introduce different LCE materials that show actuation behavior and explain how they can be synthesized. In the second part, we focus on materials in which a shape change is triggered by a phase transition. In particular, we discuss how the chemistry of the polymeric material influences the strength and direction of the shape change. We review the efforts made to trigger the actuation event by stimuli other than temperature variation. Subsequently, we summarize preparation techniques for various sample geometries of aligned LCEs that all show actuation properties and assign them to particular applications. A short summary is given of devices that have been built in this way. In the third part, we concentrate on actuators that show deformation in an electric field without any phase transition. We start with a short introduction to ferroelectric liquid crystalline elastomers (FLCEs) and discuss molecules exhibiting these phases. Subsequently, we show how the electroclinic effect of FLCEs can be utilized to induce macroscopic deformations by an electric field.

Keywords Actuators · Ferroelectric liquid crystalline elastomers · Liquid crystalline elastomers · Miniaturization · Photoisomerization

C. Ohm, M. Brehmer, and R. Zentel (✉)
Institute of Organic Chemistry, Johannes Gutenberg University, Duesberg Weg 10-14,
55099 Mainz, Germany
e-mail: zentel@uni-mainz.de

Contents

1	Introduction	50
1.1	Preconditions for Selecting LC Elastomers	54
2	Actuators Powered by a Phase Transition	55
2.1	Designing Actuators with Defined Specifications	55
2.2	Introduction of Actuator Systems	62
2.3	LC Elastomer Devices	67
3	LCEs in Electric Fields	70
3.1	Ferroelectric Liquid Crystals and Their Networks	71
3.2	Preparation of FLCEs	75
3.3	Electromechanical Properties of FLCEs	77
4	Conclusions and Outlook	82
	References	83

Abbreviations

a	electrostriction coefficient
BCFLCE	Bent-core ferroelectric liquid crystalline elastomer
BCLC	Bent-core liquid crystal
\mathbf{c} -director	Projection of the director on the smectic layer
d_{33}	Piezoelectric constant
e	Flexoelectric coefficient
FLC	Ferroelectric liquid crystal
FLCE	Ferroelectric liquid crystalline elastomer
LC	Liquid crystal
LCE	Liquid crystalline elastomer
NI	Nematic–isotropic
P_s	Spontaneous polarization
R	Radius of gyration
S	Order parameter
s_A	Smectic-A phase
s_A^*	Chiral smectic-A phase
s_C	Smectic-C phase
s_C^*	Chiral smectic-C phase
S_x	unidentified smectic phase of higher order
T	Temperature

1 Introduction

Liquid crystalline elastomers (LCEs) are materials that combine the properties of polymeric elastomers (entropy elasticity) with those of liquid crystals (self-organization). They are the subject of several reviews and books [1–10]. Their most interesting property is the ability to change their shape reversibly after the application of a certain external stimulus. This feature was predicted by de Gennes as early

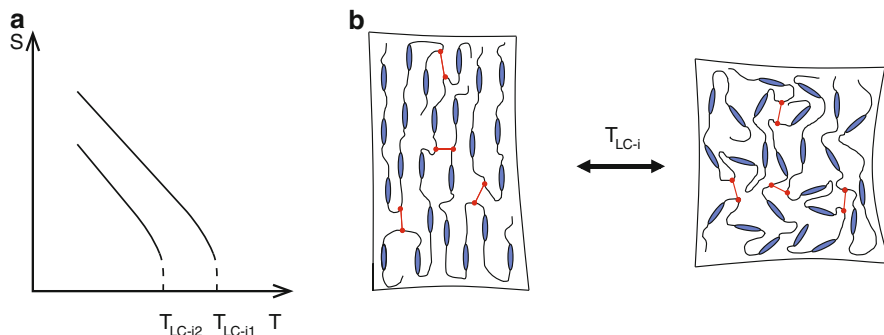


Fig. 1 (a) Anisotropy of the LC phase as expressed in the order parameter S , leads to an anisotropic conformation of the polymer backbone. The magnitude of chain anisotropy is generally assumed to have the same temperature dependence as S . It decreases with increasing temperature and jumps to zero at the clearing temperature (T_{LC-i1}). By a photoisomerization of suitable dyes (mostly azobenzene dyes) it is possible to shift the clearing temperature (T_{LC-i2}) and thus the order parameter and the chain anisotropy at constant temperature. (b) Visualization of the change of the order at the clearing temperature. In the isotropic phase the polymer chains adopt a random coil conformation, leading to a macroscopic deformation of the sample

as 1975 [11, 12]. Since then, LCEs have been extensively discussed as materials for actuators. They offer an alternative to piezoelectrics, hydrogels, and various other types of polymer systems (see [13] for an overview). The possible applications are wide, and range from micromechanical systems [14] (in atomic force microscopy, as valves in microfluidic systems, as artificial muscles in robots) to propulsion systems [15] (inspired by cilia in nature), and active smart surfaces that can change their properties according to the environment [16].

The basic idea behind the shape variation of LCEs is straightforward [184]. Imagine a network swollen with an LC material. The polymer chains experience an anisotropic environment and deviate from the isotropic conformation. As a result, the coil dimension (the radius of gyration R_G) will be different parallel and perpendicular to the LC director. Such an elastomer loses its anisotropy when heated to the isotropic phase. As a consequence, an isotropic chain conformation will be regained and the sample as a whole will change its shape (Fig. 1) [10, 11, 17, 18, 184]. This scenario, which relies on the change of the order parameter S and the resulting anisotropy of the polymer chains, is used most often. Thereby, the change of the order parameter is either directly induced by a temperature variation or by an “isothermal” shift of the phase transition temperatures, which can be achieved by a photochemical isomerization of dyes [19, 20] (see Fig. 1).

Alternatively, an external (electric) field can be used to change the orientation of the LC director inside the network. The network will then reorient and produce a shape change. This effect can be observed either in LC actuators made from highly swollen nematic systems [7, 9, 21, 22, 185] or in bulk LCEs with ferroelectric phases (see Sect. 3). In LCEs with ferroelectric phases, the electroclinic effect

[23–25] can lead to a change of the tilt angle of the mesogens in chiral smectic-C (smectic-C*) or chiral smectic A (smectic-A*) systems. This causes a change of the smectic layer thickness, which in turn induces the actuation (see Sect. 3). The polymer network serves here mostly as a matrix, which transforms a “liquid-like” ferroelectric phase into a “soft solid-like” ferroelectric, which can exert permanent stress. The magnitude of the shape change achievable in this way is smaller than for systems that rely on a nematic–isotropic (NI) phase transition. But, this actuation principle has the advantage that shape variations happen in direct response to an electric field (in fact it is a piezoelectric effect) and does not require heating.

LCEs can have different topologies depending on the attachment of the mesogenic units (see Fig. 2), which is important for the magnitude of the chain anisotropy. If they are incorporated into the main chain, a large interaction between LC phase and mechanical properties is expected. If the mesogens are attached as side groups (LC side-chain polymers), their orientation is decoupled from that of the polymer chains [26]. Thus orientational correlations will be smaller than in LC main-chain polymers [10, 27].

In this chapter, we will focus on the application of LCEs that can change their shape in response to temperature, to irradiation with light, or to electric fields (either by resistive heating or by a direct piezo-like response). Compared to inorganic piezoelectric materials, LCEs show a much larger shape variation but smaller forces. Compared to gels working by reversible swelling and deswelling, they have the advantage that the shape variation does not require mass transport of solvent.

The basic principles of preparation and operation of LCEs – especially with regard to the route shown in Fig. 3a – have been described in [184]. Still, some

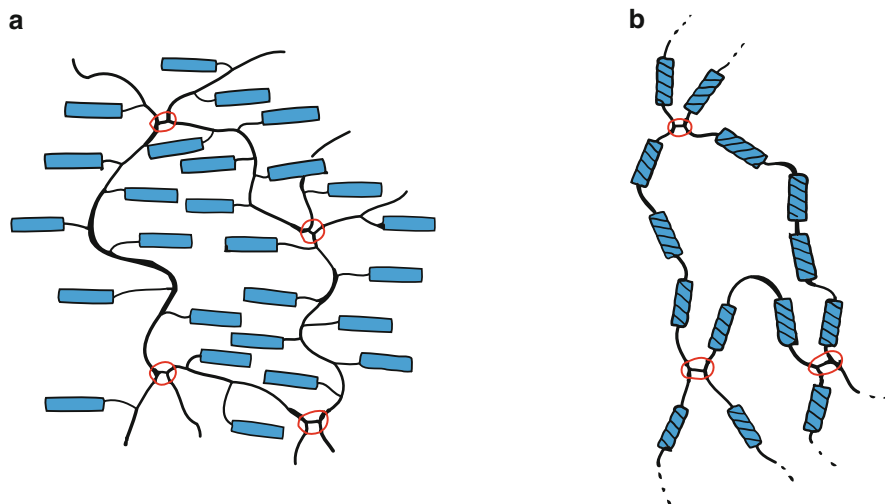
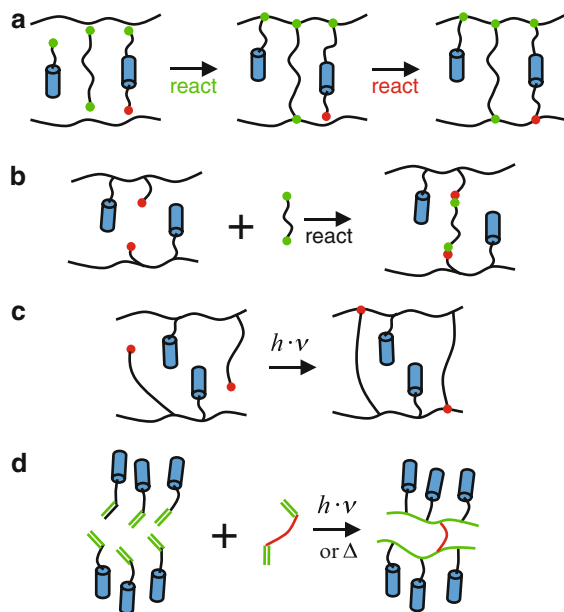


Fig. 2 (a) Network containing side-chain mesogens; (b) network containing main-chain mesogens

Fig. 3 Different reaction paths for the preparation of LCEs: (a) “One-pot” synthesis, usually via hydrosilylation; (b) reaction of LC polymer with a crosslinker; (c) LC polymer containing a reactive group that is activated by UV irradiation; (d) mono- and bifunctional low-molecular-mass LCs that are polymerized



remarks concerning crosslinked liquid crystalline polymers seem appropriate in the present context. We will discriminate between LCEs and liquid crystalline thermosets. LCEs are a subclass of chemically (or physically) crosslinked polymers with a low crosslinking density, resulting in long polymer chains between the netpoints. Thus, they can be deformed easily to high strains and they swell strongly in good solvents. Typical elastic moduli (bulk state, above the glass transition temperature T_g) are in the range of megapascals [28–31]. By contrast, highly crosslinked systems, so-called thermosets, are hard materials with little deformability that hardly swell. Their elastic moduli lie in the range of gigapascals [32]. Both types of networks can be made from LC polymers, depending on the amount of crosslinking agent incorporated. In addition, LCEs can be made by covalent crosslinking or by physical crosslinking due to the (reversible) segregation of hard or ionic blocks [33, 34]. Typical LCEs (low crosslink density) show NI phase transitions (e.g., clearing points) and a temperature-dependent LC order parameter. In LC thermosets (high crosslink density) the LC order is “frozen-in” and is nearly temperature independent, although photoisomerization can slightly change the order.

LCEs and thermosets offer differing potential applications. LCEs give rise to large deformations, which require a phase transition and strong deformability. The more densely crosslinked LC networks show small deformations, but their macroscopic shape variation can often be “boosted” by using bending deformations (see Sect. 2.3). In that case, tiny deformations at one side of an object can lead to huge bending deformations.

Additionally, it is important to realize that deformations at an NI phase transition occur locally, on the level of a small volume of the material in the micrometer range. To observe the unique properties of LCEs on a macroscopic scale, the mesogens have to be aligned uniformly over the whole sample, yielding an LC monodomain or, at least, a sample with a well-defined overall director pattern (see Chap. 1). Thus, the use of LCEs as actuators always requires a step to orient the sample prior to final crosslinking [184]. Consequently, we will discuss first the influence of different preparation strategies on the orientation step, focusing on materials for actuator applications (Sect. 1.1). This section will be followed by a discussion of properties needed for application. We will examine temperature-driven actuators (Sect. 2) and electrically driven systems (Sect. 3).

1.1 Preconditions for Selecting LC Elastomers

Generally, crosslinking can be done in various ways, as summarized in Fig. 3 and outlined in [5]. This includes a one-pot process, in which crosslinking and the build-up of the LC polymer are done simultaneously (Fig. 3a); the crosslinking of functional LC polymers with a bifunctional crosslinking agent (Fig. 3b); the photochemical crosslinking of a properly functionalized LC polymer (Fig. 3c); or the (photo)polymerization of a mixture from a liquid crystalline monomer and a crosslinking agent (Fig. 3d). For chemical crosslinking of a multicomponent mixture a solvent is needed to ensure miscibility of all components. This applies to routes (a) and (b) but it is especially important for route (a), in which the miscibility of various low-molar-mass compounds with a polymer must be ensured [184]. However, the solvent needed for this purpose will destroy the LC phase. Thus, the orientation must be accomplished in a second step, after most of the chemical reactions and a preliminary crosslinking have taken place in concentrated solution. Thereafter, the dried, solvent-free sample (now in its LC phase) is finally crosslinked in a strongly stretched state. By this method, nice macroscopic films of LCEs can be made (centimeter size), which have been the basis for most investigations in this field [184]. However, the samples made by route (a) show non-Gaussian behavior [35]. Additionally, small micrometer-sized samples with complex director patterns are difficult to make by this technique.

Orienting small samples and creating complex director patterns can be accomplished more easily by either using the orientability of the LC phase from the beginning or using electric (magnetic) fields or surface forces. This requires orienting and photocrosslinking of multifunctional LC polymers [36–39] or monomers in the neat (solvent-free) LC state [32, 40] (see Fig. 3c, d). In this case, it is either necessary to incorporate photocrosslinkable groups (route c) into the LC polymer or to establish (route d) a mixed system of (photo)polymerizable LC monomers. Route (c) has the advantage that the crosslinking of a small amount of crosslinkable groups has only a minor influence on the phase type and phase transition temperature. However, in this case the relatively high viscosity can create problems.

Route (d) has the advantage of a low viscosity of the monomer mixture. However, it is not trivial to obtain a system in which phase type and temperature range of the LC phase of polymer and monomer overlap well. From the synthetic side, either acrylate groups (photoinitiated radical polymerization) can be incorporated into an LC polymer by a polymer-analogous reaction [23, 36, 39, 41] or groups leading to direct photocrosslinking can be used, like benzophenone units [42, 43]. As a result of these efforts, neat (i.e., solvent-free) LC materials have become available, in which a complex director pattern can be created by the methods known from low-molar-mass LC systems. The resulting director patterns can afterwards be stabilized by photoinitiated crosslinking. As photocrosslinking can be done in a spatially resolved manner, this route allows the creation of different director patterns in different parts of the sample.

An interesting alternative to covalent crosslinking is the use of secondary interactions like ionic interactions [34] or complex formation [44–46]. Redox reactions that change the valence of the center ion can be used for reversible crosslinking. Also, block copolymers have been used for the formation of supramolecular networks [33, 47]. In this case, the crosslinks are formed by hard polymer segments that are in the glassy state surrounded by LC polymer segments. If such a block copolymer is heated above the T_g of the hard segments, it becomes melt-processable. As with ionic systems, the crosslinking of the block copolymers is reversible and reuse becomes possible. In the case of the covalent networks mostly investigated, recycling is not an option, as there is no way to selectively break the chemical bonds formed during preparation.

2 Actuators Powered by a Phase Transition

2.1 Designing Actuators with Defined Specifications

In this section, we will discuss LCEs in which shape variation is induced by a change of the order parameter S . This is most pronounced in the vicinity of an NI phase transition (see Fig. 1 and Sect. 1). In addition, we will discuss how the size and shape of aligned (and therefore actuating) LCE samples can be controlled in order to meet certain specifications dictated by an application. We will address the question of how the mechanical and actuation properties of the materials are influenced by the chemical nature of the LCE system.

From an application-based point of view, the most important characteristics of an actuator are the stimulus under which actuation occurs, the direction of actuation, the maximum displacement that can be produced, and the maximal force that can be created. The maximum displacement and force that an LCE actuator can produce depend on the chemical structure of the material. This aspect will be discussed in Sect. 2.1.1. Concerning the stimulus leading to the shape change, temperature-driven and UV-driven systems can be distinguished. In both

cases, the transition from the LC phase to the isotropic phase triggers the actuation. UV-driven systems contain photosensitive dyes that allow isothermal isotropization by UV irradiation. Additionally, temperature-driven systems have been coupled with other materials that allow the production of heat, either directly inside the sample by an electric current, by a magnetic field, or by infrared irradiation. The whole concept triggering the actuation will be discussed in Sect. 2.1.2. Finally, the direction in which a deformation occurs depends on the orientation pattern of the LC material. This topic will be addressed in Sect. 2.1.3.

2.1.1 LC Elastomer Structure and Strength of Actuation Properties

LCEs gain their actuation properties from the coupling between the elastomeric network and the LC units. It causes an anisotropic chain conformation of the network polymers if the mesogens exhibit an LC phase. Accordingly, the chains adopt different radii of gyration parallel (R_{\parallel}) and perpendicular (R_{\perp}) to the director. Depending on the geometrical relation between the director and the long axis of the polymer coil, we distinguish a prolate (parallel, $R_{\parallel} > R_{\perp}$) and an oblate (perpendicular, $R_{\parallel} < R_{\perp}$) conformation (see Fig. 4) [10, 48–50].

At the phase transition to the isotropic state, the polymer chain changes into a spherical conformation, which leads to a reversible shape change. The strength of this effect depends directly on the magnitude of chain anisotropy in the LC phase and is therefore a function of the coupling between polymer chains and mesogens. The architecture of the LC polymer (main-chain, side-on, end-on) has a strong impact on this coupling behavior.

Two ways of coupling are possible, namely “through bond” due to the chemical linkage between mesogens and polymer chain, and “through space” [10, 28, 48, 49]

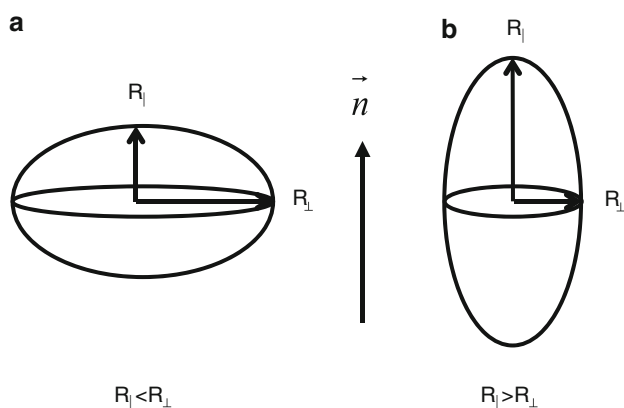


Fig. 4 (a) Oblate chain conformation: the long axis of the polymer chain is perpendicular to the director. (b) Prolate chain conformation: the long axis of the polymer chain is parallel to the director [5]. Copyright Wiley-VCH Verlag GmbH & Co. KGaA. Reproduced with permission

caused by the anisotropic environment created by the alignment of the mesogens. For LC polymer architectures in which the long axes of the mesogens are parallel to the polymer backbone (main-chain, side-on), both effects act in the same direction and cause a strong elongation of the chains parallel to the director (prolate conformation). Comparing the two systems, we find that main-chain polymers show stronger chain anisotropy than side-on systems. The reason is that the “through bond” coupling in the main-chain architecture is stronger, because the mesogens are directly incorporated into the polymer backbone. Decreasing the spacer length of a side-on system (giving it more main-chain character) increases the coupling between mesogen and backbone and thereby increases the chain anisotropy [28, 51].

In the case of end-on systems, the “through bond” coupling induces an elongation of the polymer chains perpendicular to the director, while the “through space” coupling prefers a parallel extension of the chains. This conflict concerning orientation leads to weaker chain anisotropy in end-on systems than in the two other architectures. The direction in which the backbone elongates depends on many factors, like the nature of the LC phase (nematic or smectic), the spacer length, and the chemical structure of the backbone polymer [28]. Concluding, we expect the strongest backbone anisotropy for main-chain polymers, followed by side-on and then end-on systems. Using D-NMR and small-angle neutron scattering (SANS) [50–58], it was indeed shown that the degree of backbone anisotropy decreases for the three architectures in the order main-chain > side-on > end-on.

Because the shape-changing effect has its origin in the deformed polymer chain conformation, we expect the strongest shape change in main-chain systems, and the weakest one in end-on systems. This prediction has been confirmed by comparing the shape-changing capabilities of three prominent LCE systems with different architectures (see Fig. 5). The main-chain elastomer by Ahir et al. [47] changes its

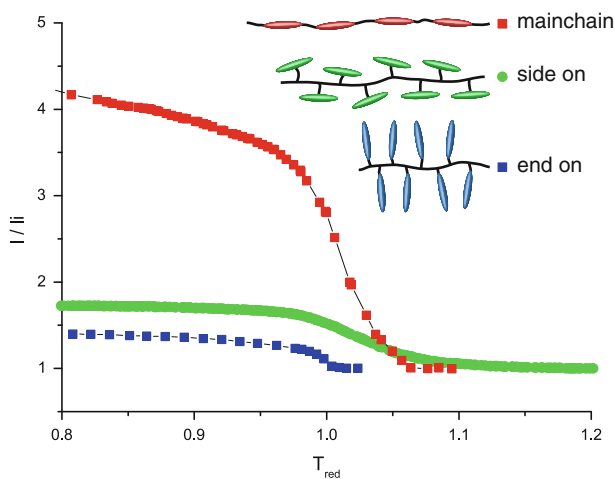


Fig. 5 Comparison of the contraction in the direction of the director for different polymer architectures. Data were taken from [18, 47, 59]

length by roughly 400% during the shape transition. The sample with a side-on architecture by Keller and coworkers deforms by 70% [59], and the end-on system by Wermter and Finkelmann shows an actuation of 40% [59]. Other samples investigated follow this trend. Additionally, the groups of both Finkelmann and Terentjev showed that the shape-change effect can be drastically increased by adding main-chain polymers to side-chain elastomers [60, 61].

Apart from the coupling between backbone and mesogens, the nature of the LC phase also has impact on the shape-changing properties. The examples presented so far were nematic LCEs. The situation in smectic LCEs is much more complex and a clear picture has not yet emerged. In fact, both poorly actuating and strongly actuating systems have been found, depending on the chemical nature of the system. This could be related to the fact that there is little information on the “quality” of the smectic layering. In addition, smectic order might be reduced by the crosslinking reaction [186]. As a first guess, highly ordered (low-temperature) smectic phases should induce a large anisotropy of the chain conformation. However, far too little SANS data exist to verify this assumption. For smectic LCEs, the deformation at the transition to the isotropic phase would be expected to be larger than for nematic ones. However, in most cases smectic LCEs possess weaker actuating properties than their nematic counterparts. Smectic-A main-chain elastomers prepared by Beyer et al. deformed by only 40% [62]. Smectic-A side-on samples by Komp and Finkelmann showed shape changes of 14% [63], and smectic-A end-on elastomers by Nishikawa and Finkelmann deformed by only 12% [64]. On the other hand, Sanchez-Ferrer and Finkelmann recently reported an example that contradicts this general trend [65]. Using two different mesogens, one of them with bulky side groups that destabilize the smectic phase, and the two-step crosslinking process, smectic and nematic main-chain polymers were prepared with nearly identical structures. In this case, the smectics showed a stronger shape variation (210%) than the nematics (80%), which was explained by the higher order parameter of the smectic phase. Finally, some smectic LCEs prepared from “diluted polysiloxanes” [36–38, 66] show no shape change at all at the phase transition to the isotropic phase [67]. The situation is complicated by the fact that in smectic LCEs the relaxation times are often rather large and in some cases the shape-changing effect was irreversible if no retracting force was applied [68].

A third parameter that impacts on the strength of the shape-changing effect is the crosslink concentration of the elastomeric network [184]. An increase in the crosslink density of nematic side-on elastomers decreases their actuation properties [69]. This is mainly due to a stiffening of the elastomeric network, thus making larger forces necessary to deform the sample. Additionally, crosslinking moieties usually produce defects in the LC phase, thereby reducing its order parameter and chain anisotropy [70, 186]. This constraint is especially important in networks from LC-polysiloxanes prepared according to the route shown in Fig. 3a. LC-polysiloxanes are usually prepared from commercially available prepolymers, which have only a modest degree of polymerization (around or below 100). This makes the use of larger amounts of crosslinking agents necessary to obtain properly crosslinked elastomers with low sol content.

2.1.2 Triggering the Actuation

All actuators discussed in this section depend on a transition to the isotropic phase to trigger a deformation. This results from the interest in large deformations, which require a considerable change of the order parameter (exceptions are bending deformations, described in Sect. 2.1.3). The phase transition to the isotropic phase always occurs at a specific temperature that needs to be controlled in order to produce applicable actuating devices. In most cases, a low transition temperature is desired, slightly above ambient conditions, as this is energy efficient and facilitates the construction of devices.

Phase transition temperatures can be influenced by several parameters. The main impact is exerted by the chemical structure of the mesogenic molecules. Stiff and highly symmetric mesogens have high transition temperatures [27, 71] and need to be avoided. For example, Beyer et al. introduced a bulky, lateral bromide group to a main-chain mesogen to suppress crystallization and to reduce the NI phase transition temperature [62]. Also, the flexibility of the polymer backbone has an influence. Highly flexible polymers like polysiloxanes yield LCEs with low glass and phase transitions, which is one reason for their popularity. Another possible way to reduce the transition temperature is by mixing two or more mesogenic molecules within the LCE, yielding a statistic copolymer [59].

Heating the whole device in order to induce actuation is impractical or even impossible for most applications. Accordingly, there is a demand for methods that produce heat directly inside the LCE without affecting its surroundings. Most straightforwardly this can be achieved by integrating a resistive wire into the sample and applying an electric current [72]. The resulting heat leads to a NI phase transition inside the material, triggering a deformation. Evidently this is not a method of choice. A more sophisticated principle was applied by Chambers et al. [73], who incorporated carbon black into the LCE sample, making it conductive by itself. Applying an electric current through the sample creates a temperature increase that initiates a shape change. It is, however, the weak point of these approaches that they require a composite material made from a “shape-changing” compound (LCE) and a “not-shape-changing” compound (the conducting material). Deformations (shape changes) create stress and lead, after repeated actuation, to delamination and a loss of the percolation of the conducting particles.

Alternatively, single-walled carbon nanotubes have been mixed into the LCEs [74]. They were, however, not used for conduction, but because they possess a strong absorption for infrared radiation and the visible spectrum. Thus, irradiating the sample with infrared light can create enough heat to induce the transition to the isotropic phase. Since this process does not require percolation of the carbon nanotubes it is much less sensitive to shape variations.

Magnetic fields have also been used to heat the actuating material directly. For this, Kaiser et al. introduced magnetic iron oxide nanoparticles into an LCE sample [75]. In a quickly changing magnetic field (300 kHz) the continuous reorientation of the magnetization produces heat, which induces a shape change.

For some applications, the production of local heat might be undesirable. In these cases, an isothermal NI phase transition induced by UV irradiation might be a suitable choice. The *cis*–*trans* isomerization of mesogens containing a photo-isomerizable group (mainly azobenzene Ph–N=N–Ph) changes their shape from rod-like to kink-like. This leads to a destabilization of the LC phase [19, 62, 76], reducing the transition temperature to the isotropic phase and thus causing isotropization at a constant temperature [20]. The concept can be transferred to LCEs in two ways. Either an LCE network is swollen with the azo compound [77], or azo-containing mesogens are covalently attached to the polymer backbone [19, 62, 78–80]. Figure 6 shows the actuation properties of an LCE film with covalently incorporated azo-mesogens in different concentrations in dependence of temperature and UV-irradiation state [80]. Both increasing the temperature and irradiating the sample produces a contraction of roughly 20%. After the shape change, irradiating the sample with visible light accelerates the re-isomerization of the azo groups, thus making the actuation reversible. The wavelength under which the isomerization occurs can be influenced by substitution of the azobenzene with functional groups that increase the length of the conjugated π -system. Examples are amino-nitro azobenzene and azotolane, which have absorption maxima close to the wavelength of visible light [81]. For further discussion on this topic see [187].

2.1.3 Modes of Actuation: Contraction, Expansion, and Bending

In Sect. 2.1.1 we pointed out that the direction of actuation relative to the director depends on the architecture of the LC material. Systems with a prolate chain conformation (main-chain and side-on) show a contraction parallel to the director, whereas LCEs with oblate backbones (many end-on systems) expand in this direction. Due to the necessity to retain a constant volume, the LCE sample compensates this deformation by expanding or contracting in the direction perpendicular to the director.

The situation becomes more complex in samples that are not aligned in a classical monodomain (in which the director is uniform over the full sample volume), but in a defective structure. An example is provided by films constrained by two different alignment layers at each side: one that facilitates a planar orientation and one that produces homeotropic alignment. In such films the director is aligned in a splay-defect structure. During the NI phase transition a bending deformation occurs [82]. A similar effect takes place in thick UV-responsive samples if the dye concentration is high enough. Due to the strong absorption, the UV light does not penetrate through the whole film thickness. As a result, the shape change is concentrated at the incident surface. This leads to a bending of the whole film [40, 83].

Complex director field alignment also occurs in very small or strongly curved samples. Nanometer-sized colloids from LC polymers and elastomers prepared by emulsion polymerization can show a bipolar, concentric, axial, or radial director field configuration, depending on their preparation method [84, 85]. During the NI

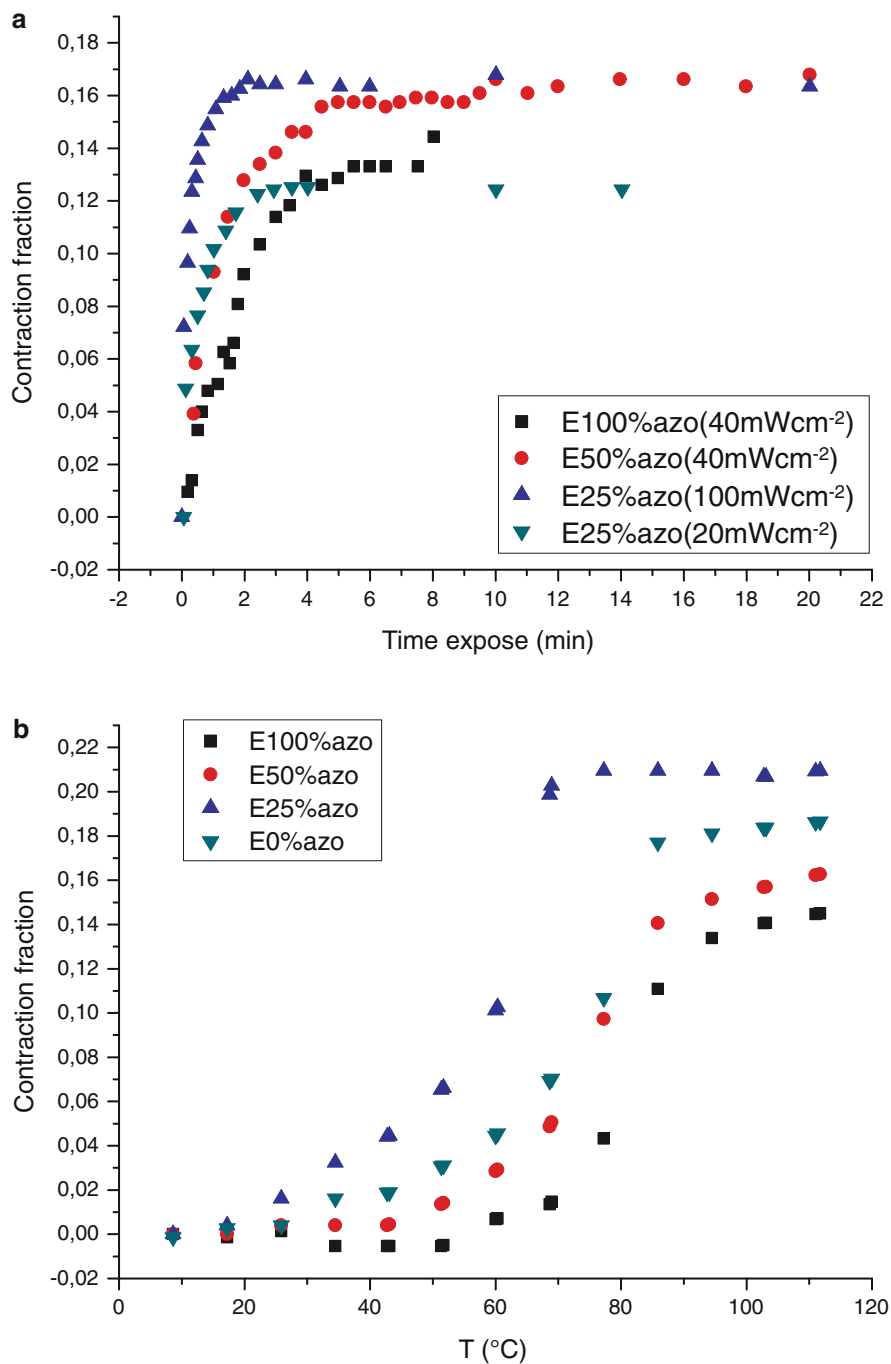


Fig. 6 Shape change of an LCE containing different concentrations of an azobenzene dye: (a) by exposition to UV light and (b) by changing temperature [80]

phase transition, such samples show different types of deformation [86, 87]. The orientation pattern can be controlled by experimental parameters in larger particles prepared by polymerization in a microfluidic system. Using different amounts of shear during polymerization, Ohm et al. succeeded in preparing two types of particle samples with a concentric and a bipolar orientation, respectively [87]. Upon heating through the NI phase transition, the concentric alignment produces an expansion perpendicular to the symmetry axis while the bipolar samples contract.

2.2 Introduction of Actuator Systems

We will discuss several strategies to tether the properties of LCE actuators to certain specifications, and then present examples of actuator systems of different shapes and different domain sizes. We shall differentiate between macroscopic and microscopic LCE actuators. Films (Sect. 2.2.1) and fibers (Sect. 2.2.2) typically have at least one macroscopic dimension. Microscopic actuation systems from LCEs have received much interest lately and have recently been the subject of a specialized review [88]. In Sect. 2.2.3, we will discuss micrometer-sized actuators that are fixed on a solid substrate to yield stimuli-responsive surfaces. In Sect. 2.2.4, we will review several methods for preparation of colloid-like actuators that are freely suspended in air or in a surrounding liquid.

2.2.1 Film Samples from LC Elastomers

The concept of actuation in aligned LCEs was first demonstrated in film samples. Uniform orientation was achieved by mechanical stretching [89] of pre-crosslinked films and subsequent full crosslinking under a load [18, 90, 91]. The shape change of such a film is displayed in Fig. 7a. Subsequently, techniques using magnetic fields [33] and uniform substrate layers [40, 59, 80, 92, 93] were utilized to achieve alignment without the need for the two-step crosslinking procedure. In these cases, the films were usually prepared on solid substrates and released after polymerization by a sacrificial layer. An example of that kind of specimen is given in Fig. 7b. Due to the flat geometry, films allow a defect-free director pattern leading to an LC monodomain with a high value of the order parameter. This results in strong deformations during the NI phase transition.

LCE films typically have lateral dimensions of several centimeters and a thickness of hundreds of micrometers. This large size makes the samples ideally suited for mechanical testing as well as for X-ray investigations. Accordingly, most fundamental studies have been carried out on such films. One disadvantage of film samples is the large amount of LC material often needed. This has been overcome by a technique introduced by Ikeda and coworkers [94]. By laminating a thin layer of aligned LCE material onto a nonresponsive plastic film, a composite

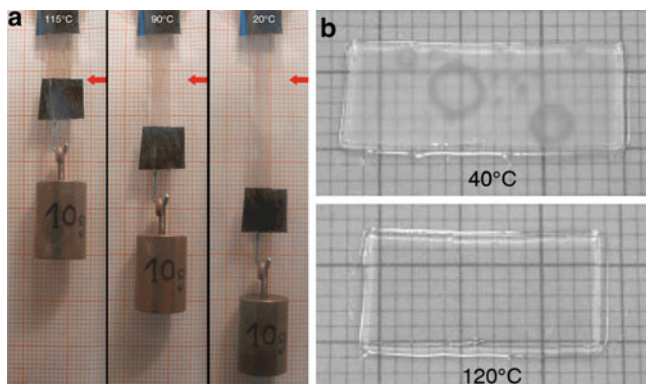


Fig. 7 (a) LCE film sample oriented by mechanical stretching with a small weight attached. Increasing the temperature results in a contraction of the film, lifting the weight [60]. (b) Film sample oriented by a magnetic field. During the contraction the film shows a deformation [33]. Copyright Wiley-VCH Verlag GmbH & Co. KGaA. Reproduced with permission

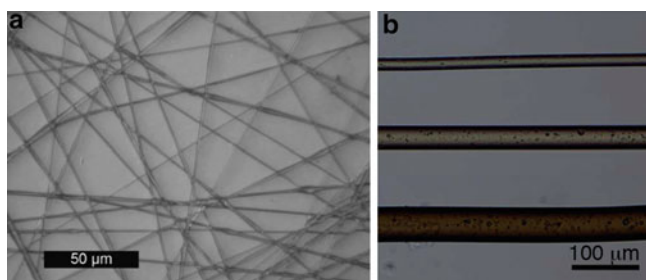


Fig. 8 (a) Fibers from a LC elastomer prepared by electrospinning and cast on a substrate [95]. Copyright Wiley-VCH Verlag GmbH & Co. KGaA. Reproduced with permission. (b) LCE fibers with different diameters prepared by a wet spinning process [68]. Reproduced by permission of the Royal Society of Chemistry

sample is obtained. At the NI phase transition induced by UV irradiation, a bending deformation occurs due to a shape change in the LCE layer only (compare with a bimetal film with different expansion coefficients). Additionally, the composite sample has superior mechanical stability compared to pure LCE films. (Fig. 8).

2.2.2 Fiber Samples from LC Elastomers

Due to their shape, fibers from LCEs closely resemble “artificial muscles”. They are typically made by extrusion of a reactive LC pre-polymer, either from solution or from the melt, followed by crosslinking. During extrusion, strong shear forces act on the polymer chains and most polymers show alignment under these conditions [96]. For LC polymers the effect is even stronger, resulting in a high degree of

orientational order within the fibers. Usually, the polymer chains are elongated in the direction of the fiber axis. Consequently, the director is aligned parallel to the fiber axis for prolate LCE systems and orthogonal for oblate systems.

The most common way to make fibers is by drawing them manually with tweezers from a polymer melt [41, 97]. The technique is very easy to perform and requires only small amounts of material. Disadvantages are the limited length of the fibers and the poor amount of control over their diameter. Even so, it has developed into a standard method for preparation of samples for X-ray diffraction and thermomechanical experiments. A more sophisticated method is electrospinning [47, 95], whereby a polymer solution is drawn continuously from a thin nozzle by an electric field and is crosslinked at the same time. This results in very thin and highly oriented fibers with diameters of 0.1–5 μm that can be cast onto a substrate. Because of their high tensile strength, there is some similarity between these fibers and natural spider silk. During the NI phase transition the fibers show a contraction. Possible fields of application are microactuation and textiles. A third synthetic technique is wet-spinning in a microfluidic setup, which yields fibers with diameters of 20–50 μm [68]. In this case, the polymer solution is injected into the flow of a second fluid, which mixes with the solvent of the polymer, leading to precipitation. The resulting fiber can be crosslinked continuously by UV light and rolled up. This yields infinitely long oriented fibers with a diameter controlled by the flow rates of the two phases. In a demonstration experiment, a small weight was attached to such a fiber, which was subsequently heated above the NI transition temperature. Across the phase transition a reversible rising of the weight was observed. Hence, the authors concluded that this technique is suitable for preparing specimen for mechanical testing.

2.2.3 Stimuli-Responsive Surfaces

Patterning surfaces with micrometer-sized objects from aligned LCEs is an interesting objective because such stimuli-responsive surfaces allow manipulation of properties like wetting behavior or adhesion on demand. Secondly, creating micrometer-sized structures from LCEs directly on a solid substrate allows their incorporation into micro-electromechanical systems (MEMS) or microfluidic lab-on-chip systems where they can serve as valves, switches, or mixing devices. Due to its simplicity, LCE-based actuation offers strong advantages over conventional motors, if small devices are required.

Keller and coworkers used soft-molding to produce micrometer-sized cylinders attached to a solid substrate [16]. To achieve this, a polydimethylsiloxane (PDMS) mold with a negative of the desired pattern was pressed onto a thin film of a molten, nematic side-on monomer on a solid substrate. After aligning the mesogens in a magnetic field, polymerization and crosslinking were initiated by UV irradiation through the PDMS mold. When the mold was peeled off, a surface consisting of regular cylinders from aligned LCEs was obtained. During the NI phase transition, the cylinders showed a reduction in length. The same procedure has been performed

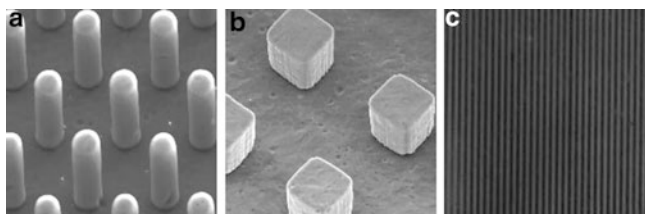


Fig. 9 Micrometer-sized patterns from aligned LCEs on a substrate: (a) cylinders [16], (b) cubes [16], (c) lines [93]. (a, b) Reprinted with permission; copyright (2009) American Chemical Society. (c) Reproduced by permission of the Royal Society of Chemistry

with another monomer system that yielded main-chain LCEs upon polymerization [16]. Compared to the first example, this drastically increased the strength of the pillar's response at the phase transition up to an impressive value of 400%. Accordingly, smart materials have been obtained that allow manipulation of their surface roughness by an external stimulus. Possible applications of such single pillars are valves and micropumps in microfluidic systems.

Ellias et al. used an approach based on photolithography to produce similar stimuli-responsive surfaces [93]. A layer of a photopolymerizable nematic material was spin-coated on a plasma-treated glass substrate and irradiated through a photomask. After dissolving the unexposed areas, the glass slide was covered with a regular pattern of LCE material. Due to the plasma treatment, the mesogens align homeotropically on the strongly hydrophilic substrate, yielding a director orientation perpendicular to the surface. During the NI phase transition, a reversible contraction of the micrometer-sized features was observed (Fig. 9). Van Oosten et al. applied an ink-jet printing approach to prepare micrometer-sized objects from aligned LCEs on a solid substrate [82]. A polyvinylalcohol (PVA) sacrificial layer was spin-coated on a substrate, followed by an alignment layer from polyimide. Two different LC monomers were ink-jetted on top of this assembly and were polymerized and crosslinked by UV irradiation. Dissolving the PVA yields freestanding cantilevers that are attached to the substrate by only their end. UV irradiation of different wavelengths initiates a reversible bending of these structures in different directions. Mimicking natural cilia, the movement of the cantilevers could be used as a propulsion system for microdevices in a fluid environment. Also, microfluidic devices seem possible in which the bending motion of the cantilevers is utilized to generate a turbulent mixing flow.

2.2.4 Freely Suspended Micro- and Nanometer Particles from LC Elastomers

A different aspect of micro-actuators is their synthesis as freely suspended objects in a fluid environment. The advantage of this concept is that it allows simultaneous application of many actuators with identical size and shape. If the micro-objects are aligned via self-assembly, their sheer number can create strong deformation forces.

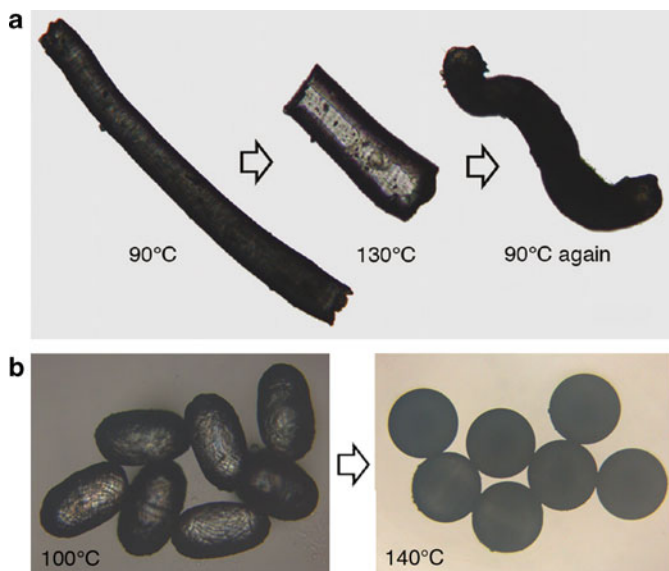


Fig. 10 Thermoactuation of LCE microparticles prepared in a microfluidic setup. *Top*: fiber that shortens during actuation [87]. *Bottom*: spheres that become rods [98]. (a) Reprinted with permission; copyright (2011) American Chemical Society. (b) Copyright Wiley-VCH Verlag GmbH & Co. KGaA. Reproduced with permission

Ohm et al. used microfluidic techniques to prepare micrometer-sized particles with different shapes from LCEs (Fig. 10) [98]. A molten nematic monomer is injected through a thin needle into a flowing stream of an immiscible carrier fluid. This results in the continuous formation of equally sized monomer droplets. These droplets are flown through thin tubes giving them the shape of spheres, disks, or rods and inducing an ordered director field [87]. By irradiating the droplets with UV light, polymerization and crosslinking is initiated, thus permanently fixing their shape and the internal orientation. When heated, the resulting particles show a reversible deformation. Control could be achieved over different parameters of the micro-actuators, like size, strength of the shape variation, and the direction of actuation (both expansion and contraction). The high level of control over the particle's physical properties allows production of actuators for specialized applications. Possible fields of interest are microlenses, valves on microfluidic chips and displacement devices [69].

Actuators of an even smaller size scale have been prepared by two groups using anodized aluminum oxide (Alox) as a template [99, 100]. In both cases, the regular, cylindrical cavities formed during the anodic oxidation of aluminum were filled with an LC monomer that was subsequently polymerized and crosslinked by UV irradiation. Afterwards, the template was dissolved by wet chemistry and regularly shaped LCE rods with a diameter of hundreds of nanometers and a length of several micrometers were obtained. Due to surface effects within the Alox template, the director was aligned parallel to the long axis of these nanorods. This orientation was

exploited by Cairns et al. to rotate these objects in electric and magnetic fields [99]. Possible applications are rheological fluids. Ohm et al. performed thermomechanical experiments whereby the rods showed reversible actuation on a size scale between the micro- and nanometer region [100].

The smallest defined structures from LCEs have been prepared by miniemulsion polymerization [86]. A main-chain polymer was emulsified by ultrasonication in an immiscible fluid and photocrosslinked in the LC state. The resulting particles were spherical with diameters of 50–300 nm. Upon heating inside an electron microscope the spheres transformed into rods and platelets, thus demonstrating the concept of actuation on a nanometer scale. An interesting question is whether the stimulus-triggered shape change of such suspended colloids also has an impact on the properties of the surrounding medium. If this is the case, fluids with a switchable viscosity might be accessible.

Yang et al. used the same method to prepare particles from noncrosslinked LC polymers [101]. The shape of the obtained nanoparticles was found to deviate from spherical. Such shape-anisotropic colloids are usually very difficult to produce by miniemulsion techniques.

2.3 LC Elastomer Devices

We will now discuss devices based on phase transitions within LCEs. This section will not only deal with weakly crosslinked elastomers, but also with liquid crystalline thermosets. Whereas LCEs are used for linear actuation, more densely crosslinked materials find application in devices that are operated in a bending mode. Due to their higher mechanical stability, the number of examples for materials that show flexure is much larger. Their mechanical properties can be enhanced by coating the LC material on a flexible substrate [94]. The preparation of such devices is easy, as standard procedures for thin film preparation or ink jetting can be used. Another advantage of thin films is the contact-free addressing by light [102]. This is not possible in thicker films, in which an intensity gradient throughout the sample inhibits a uniform deformation.

Light-induced flexing can be used to move objects on surfaces. Finkelmann et al. prepared dye-doped LCE stripes that bend upon irradiation due to a director dislocation [77]. In the dark, the sample relaxes quickly to a flat state. If such LCE rafts float on a water surface, the deformation moves them away from the illuminating beam [77]. Off-center irradiation results in a skew deformation of the LCE allowing directional control of the movement. Directed movement on solid surfaces is also possible in the case of an asymmetric design of the actuator (Fig. 11) [103]. For an LCE covered stripe a change of flexure can be induced. Different edges allow changing the stationary point and enable an inchworm-like movement in one direction. Switching the dye in the sample from the *trans* to the *cis* state and back controls the curvature of the stripes. This shape change is achieved by alternating irradiation with UV and visible light.

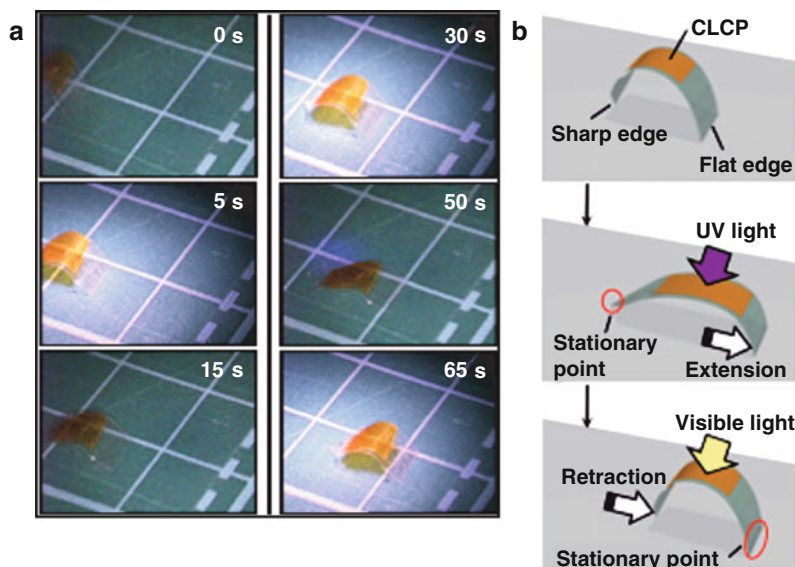


Fig. 11 Moving stripe of a composite of polymer film and LCE. [103]. The photoisomerization of the incorporated azo dyes controls the bending. The direction of the walk depends on the shape of the edges. Reproduced by permission of the Royal Society of Chemistry

Using an LCE-coated ribbon, the group of Ikeda has been able to construct a light-driven motor [94]. The belt is put around two pulleys with different diameters. Upon irradiation on one side with UV light and the other side with visible light, the pulleys is made to rotate due to the consecutive contraction and extension on the two sides. (Fig. 12)

The aforementioned examples of bending devices work digitally with two different states. For other applications it might be necessary to have various different bending angles. Such a variable bending can be achieved by a gradual distortion of the director in the LCE with the help of shape-changing molecules [104]. Consecutive *trans*–*cis*–*trans* isomerization of azo compounds induced by polarized light leads to a rotation of the dye out of the polarization direction [105, 106]. In this way, a change of the polarization direction leads to a gradual change of the LCE's order and thus the flexure [104].

Cilia are hair-like objects that work as actuators by flexing. Because of their small size they are used in arrays. They can be prepared easily by inkjet printing [82], which offers the possibility to combine polymers with different absorption wavelengths in one device. If one segment is switched by visible light and the other by UV light, different shapes can be achieved. These fibers have been attached to a surface in order to move objects (Fig. 13). Cilia could also be attached to devices that are propelled autonomically.

Recently, a miniaturized gripper that is propelled by an LCE film has been introduced [107]. Using lithographic methods, an LCE film and the silicon pincers

Fig. 12 LCE-covered ribbon moves two pulleys. Simultaneous irradiation with visible and UV light on different areas of the setup leads to contraction and expansion on different sides [94]. Copyright Wiley-VCH Verlag GmbH & Co. KGaA. Reproduced with permission

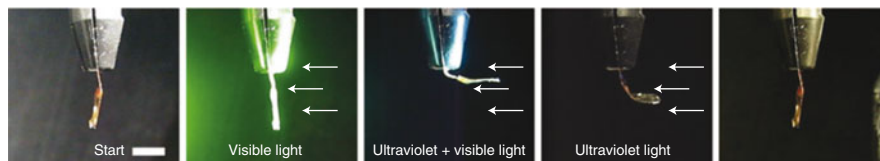
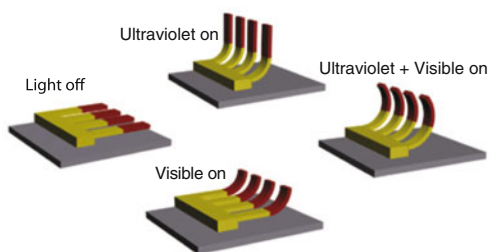
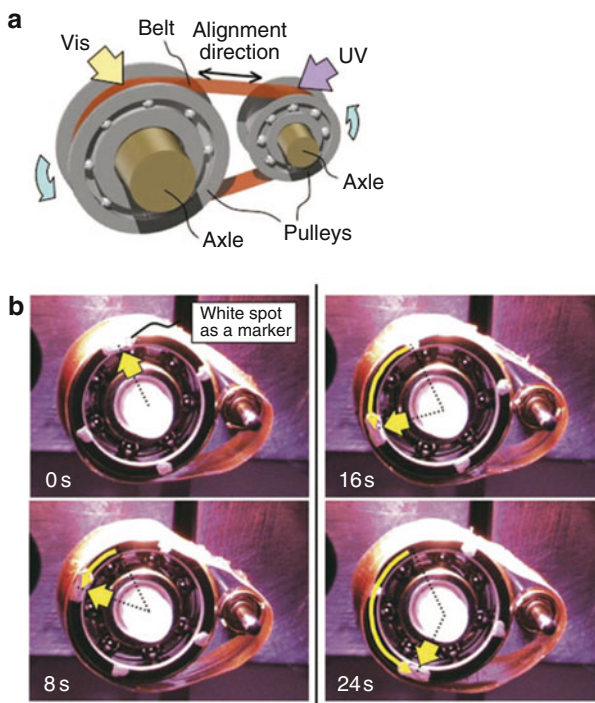


Fig. 13 Fibers containing two different LCEs sensitized to different wavelengths. Different combinations of light sources allow different movements [82]. Reprinted by permission from Macmillan Publishers [Nature Materials]. Copyright (2009)

are integrated into a micromechanical device. A gold wire is wound around the LCE, thus allowing heating of the material with an electric current. If the NI transition temperature is reached, the device can grab an object.

Mechanical deformations can also be used to obtain switchable optical elements. In the first step, lines are written into an oriented polymerizable low-molecular-mass LC by two-photon lithography. After stabilization of the support by polymerization with weak UV light, an optical grating is obtained [108]. If the grating vector is parallel to the nematic director, the distance between the lines shrinks upon heating from the nematic to the isotropic phase. This modifies the step size of the grating and a change of the diffraction pattern is observed. Hence, in this way a tunable grating is generated [109].

Solvent-dependent (chemical) applications of the LCE shape change have also been reported. They are based on a combination of (1) the well-known isotropic swelling of elastomers with (2) a strong anisotropic deformation, when the swollen network becomes isotropic. An LCE containing hydrophilic carboxylate groups changes its shape with water uptake and thus can be used as an indicator of moisture [93, 110]. Starting with an LCE with different director orientations on each side of the sample, the LCE not only increases its volume during water uptake, but also bends strongly because of the anisotropic swelling [69].

3 LCEs in Electric Fields

Reorientation of the LC director in electric fields is the basis of liquid crystal displays (LCDs). Hence, it is straightforward to think of initiation of actuation in an LC elastomer by application of an external electric field that causes reorientation of the LC director inside the elastomer. This should lead to a reorientation of the anisotropic polymer chain (see Fig. 4) which, in turn, induces a shape variation. However, all experiments performed so far demonstrate that it is not possible to transfer enough energy for a shape variation on the nematic director. Because the network topology stabilizes the sample shape and chain anisotropy present during crosslinking [4], the director of nematic LCEs cannot be switched in electric fields if the shape of the elastomer is kept fixed. By contrast, for freely suspended and highly swollen pieces of nematic LCEs, shape variations in electric fields have been observed as a response to the reorientation of the director [14, 15, 185]. However, the interaction with an electric field is much stronger for ferroelectric (chiral smectic) liquid crystals. It is possible to prepare ferroelectric LCEs in which a full switching of the director by external electric fields occurs while, at the same time, the director orientation present during crosslinking is stabilized by the network [23, 36–38].

A second possibility exists for inducing a shape variation in ferroelectric LCEs. It results from the phase transition between a smectic phase with an orientation of the director along the layer normal (s_A) and a smectic phase with tilted mesogens

(s_C^*). This transition can be induced by an electric field (electroclinic effect) and leads to a decrease in the thickness of the smectic layers, resulting in a shape variation.

3.1 *Ferroelectric Liquid Crystals and Their Networks*

We will first describe LC phases with ferroelectric properties and subsequently outline the general properties of the ferroelectric LCEs (FLCEs). The most intensely studied phase is the chiral smectic-C* phase (s_C^*) (see Fig. 14). It is the chiral modification of the smectic-C phase, a tilted smectic phase formed from chiral (pure enantiomers) rod-like mesogens. Chirality is essential because it eliminates the mirror plane present in the classical smectic-C phase. This reduces the symmetry of the phase and allows a macroscopic polarization perpendicular to the plane of the layer normal and the director, which now follows the average tilt direction of the mesogens (for an overview see [113–119]). This macroscopic dipole moment (spontaneous polarization) is a consequence of the reduced symmetry and the fact that the lateral dipole moments of individual mesogens no longer cancel each other due to a slightly biased rotation around their long axis. This symmetry argument applies to all tilted smectic phases formed by chiral rod-like mesogens. However, for higher-ordered smectic phases than s_C^* , ferroelectric switching (see Fig. 14a), which is the final proof of ferroelectricity, is difficult to perform due to the high viscosity. This problem is even more severe for FLCEs, in which the switching times can be very long [37, 38].

In summary, chiral smectic-C* phases lack a center of symmetry. Hence they can be used as materials for second-order nonlinear optics [120–124], and possess piezoelectric and pyroelectric properties. Pyroelectric measurements have been performed on LC polymers [125] as well as on LCEs [126–128]. Irradiation of an FLCE sample with light usually leads to a temperature increase resulting in a pyroelectric signal [129]. More interesting are systems in which dye molecules like azobenzenes lead to a shift of the phase transition temperature upon isomerization [19].

Furthermore, in FLCEs the macroscopic electric dipole moment provides a handle to apply a strong torque onto the director (see Fig. 14a). The resulting switching occurs on the cone of the so-called *c*-director, the projection of the director on the smectic layer plane (see Fig. 14a). Soon after the discovery of the potential of chiral smectic-C* phases, the search for LC polymers with these phases started [130–132]. However, as ferroelectric switching is the final proof for the assignment of the phase, the more closely studied ferroelectric LC polymers were limited to several LC polysiloxanes, which have a low T_g and a relatively high switching speed [25, 66, 133–136] (see Scheme 1). These polymers form the basis for most of the FLCEs discussed here.

Closely related to the chiral smectic-C* phase is the so-called chiral smectic-A* phase (s_A^* , see Fig. 14b) (for an overview see [24, 25, 119, 142, 143]). Without the presence of external electric fields, the s_A^* phase is identical to the smectic-A (s_A)

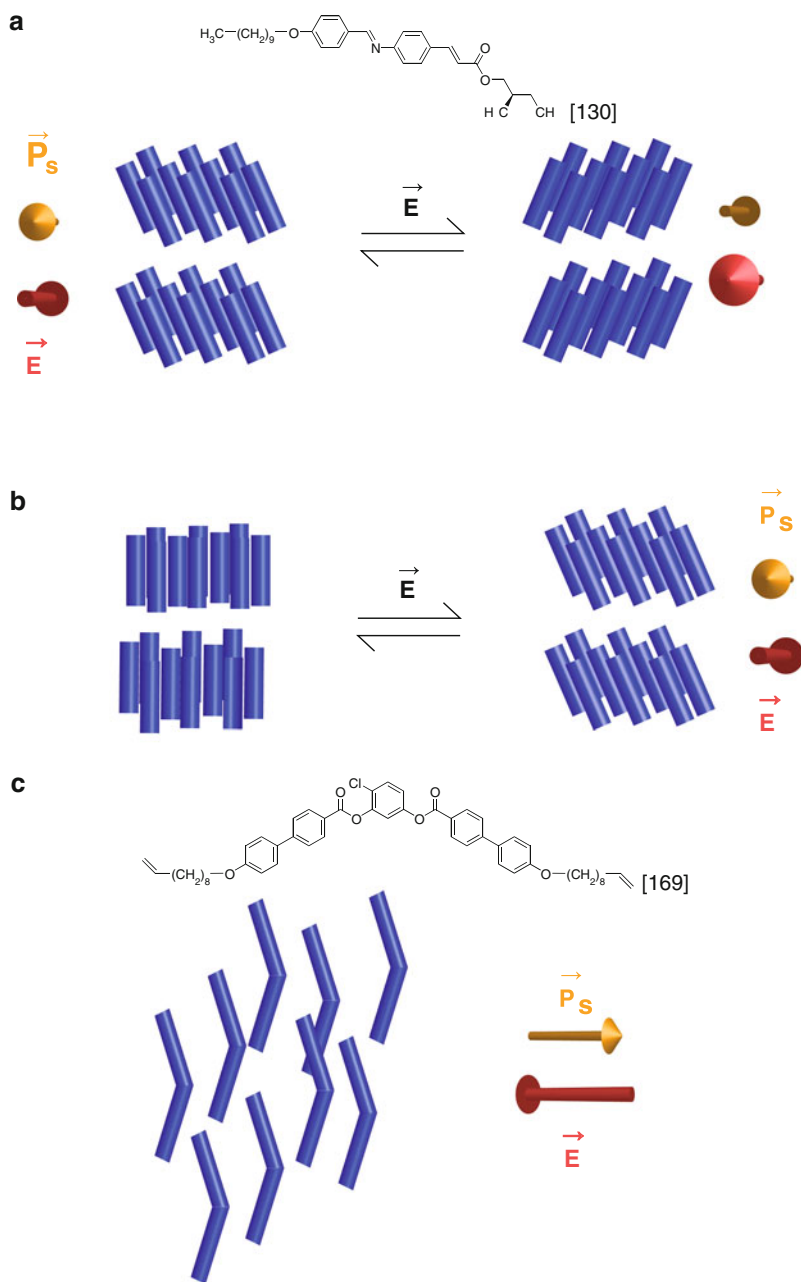
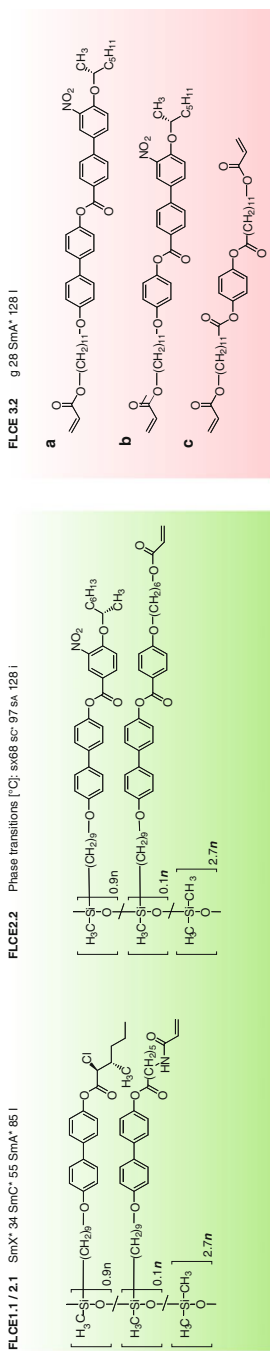
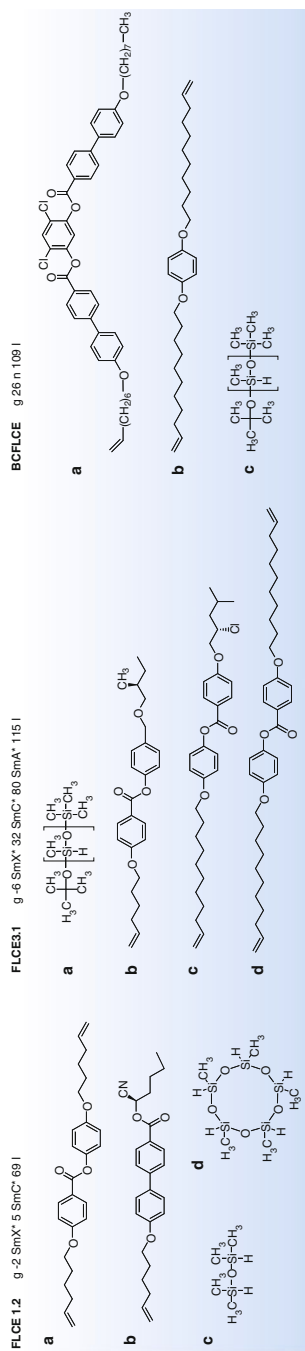


Fig. 14 Ferroelectricity in LCs. **(a)** In the smectic-C* phase an electric field (E) can reverse the tilt and thereby the direction of the polar axis perpendicular to the tilt direction. **(b)** Application of an electric field to a chiral smectic-A* phase induces a tilt of the molecules and thereby a polar structure. **(c)** In an aligned bent-core nematic phase a dipole is present in the direction of the kink. [111, 112]



Scheme 1 Starting materials for FLCEs sorted by preparation method. The phase transitions were measured for the elastomers. The data are taken from the following references: FLCE 1.2 [137], FLCE 3.1 [138], BCFLCE [139], FLCE 1.1 and FLCE 2.1 [36, 37], FLCE 2.2 [38], and FLCE 3.2 [140, 141]

phase known from achiral mesogens: the director is oriented parallel to the layer normal, perpendicular to the layer plane. However, if an electric field is applied perpendicular to the layer normal of the s_A^* phase, the mesogens tilt perpendicular to the field (see Fig. 14b). Hence the field induces a transition from an orthogonal smectic phase (s_A) to a tilted smectic phase (s_C^*). This occurs because the tilting reduces the symmetry and induces a macroscopic polarization, which can interact with the external field. This effect is strongest at the (second-order) phase transition temperature (Curie temperature) between the s_A^* and the s_C^* phase. In combination with chiral smectic elastomers, this behavior is very effective at inducing shape variation because the sample shrinks parallel to the smectic layer normal (each layer gets thinner by tilting, see Fig. 14b) while it expands in the perpendicular direction.

In addition to chiral rod-like smectics, ferroelectricity has also been observed in LC phases from bent-core mesogens. In the case of these banana-shaped molecules, the core shape, together with their dense packing, biases the rotation around the long molecular axis [144, 145]. This leads to a summation of the molecular dipoles in the direction of the kink [146–148] (see Fig. 14c). Because of their molecular shape, not only smectic phases but also biaxial nematic phases show ferroelectricity [149, 150]. In this context, one has to bear in mind that alignment of the mesogens is essential to obtain devices. Smectic materials with a low viscosity and a low phase transition temperature (like the s_C^* phase discussed above) usually meet these prerequisites better than the highly viscous polar phases of banana-shaped mesogens that normally exist at temperatures above 100°C. A recent example of a bent-core elastomer will be discussed at the end of this section.

We will concentrate here on systems in which the LC director is coupled to the network without losing its softness. This means that a rotation of the polar axis is still possible (see Fig. 14a) and real FLCEs can be prepared [23, 36–38]. Densely crosslinked systems that possess a polar axis, but cannot be switched [151–153], will be excluded. Although FLCEs can be switched, the state prior to crosslinking is stored. This is manifested in the optical hysteresis curve (see Fig. 15). The center of the curve is shifted from zero voltage in the direction opposite to that of the polarity of the field applied during crosslinking. This behavior can be explained by an additional internal mechanical field [23] that exhibits a minimum at the switching state in which the sample exists during crosslinking. This asymmetric switching is also observed in the smectic-A* phase. However, in that case the hysteresis is gone. The mesogens do not rotate between two ferroelectric states, but change their induced tilt angle due to the electroclinic effect (see Fig. 14b). Here again, the mechanical field shifts the switching curves to one side [23].

The FLCEs prepared in this way can be used either as sensor components, transforming a mechanical deformation into an electric signal, or as actuators that change their shape on application of an electric field. From the chemical point of view, they can be made by covalently linking the mesogenic groups to form a slightly crosslinked rubbery polymer network structure [3, 5, 8, 10, 154–156] or by dispersing a low-molar-mass liquid crystal in a phase-separated network structure [7, 40, 157–162]. These two systems possess very different structures locally. Macroscopically, however, they show very similar properties.

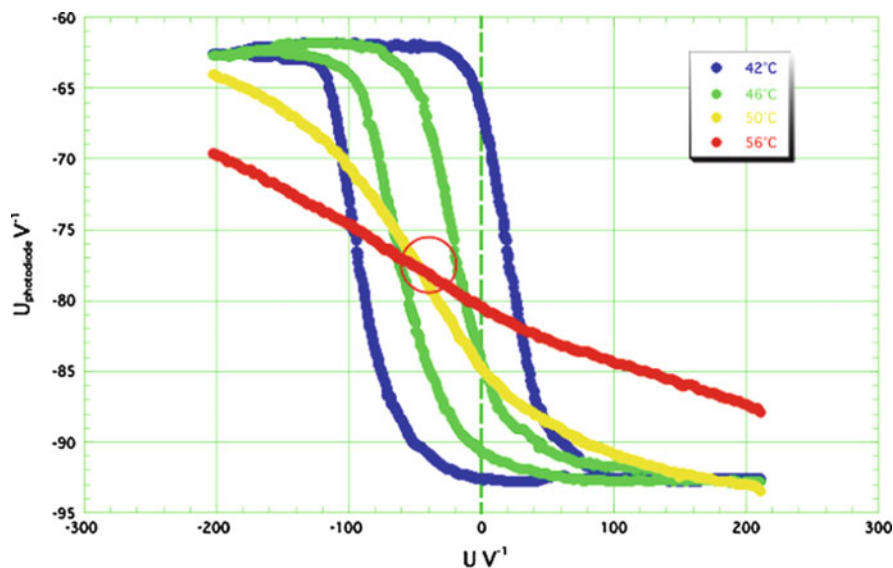


Fig. 15 Electrooptical hysteresis of a ferroelectric elastomer crosslinked in the sc^* phase [23]

3.2 Preparation of FLCEs

The outstanding property of FLCEs being their macroscopic dipole, the preparation must assure uniform alignment of the mesogens. The most direct approach to achieve this goal is application of an electric field during the crosslinking process [36]. Because the material has to be aligned prior to crosslinking at elevated temperatures, thermal reactions are inapplicable and photoinitiation becomes the method of choice. However, some photoinitiators can give ionic impurities if irradiated in the presence of an electric field. Such a side reaction renders the sample unsuitable for experiments with electric fields.

Depending on the method of preparation, different orientations of the polar axis can be realized. If the samples are aligned between indium tin oxide (ITO)- and polyimide-coated glass slides, the mesogens align parallel to the surface and the smectic layers are oriented perpendicular to the glass slides [111]. Application of an electric field leads to a polar monodomain by alignment of the director. The polar axis is perpendicular to the film, in the direction of the electrodes (Fig. 16).

In spin-coated or free-standing films, the smectic layers are aligned parallel to the surface [163, 164]. In such a homeotropic arrangement the tilt direction is not defined and the polar axis of different domains is randomly distributed over the film. If the substrate is water-soluble, it can be dissolved and freely suspended films can be obtained [165].

Alternatively, a “two-stage” mechanical orientation can be applied to obtain polar FLCEs (see Fig. 17 and [184]). A first stretching aligns the director. However,

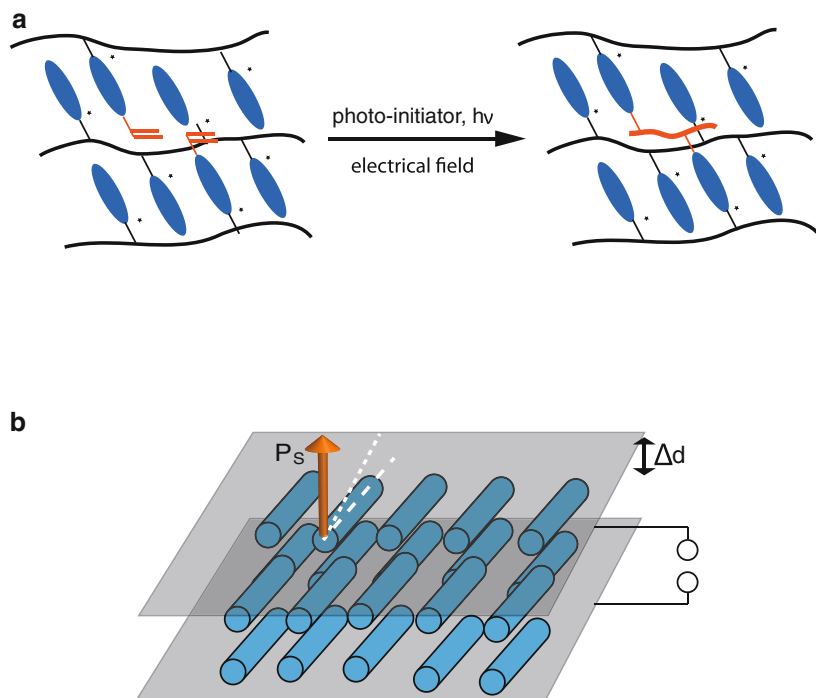


Fig. 16 (a) Crosslinking of an FLC polymer in the polar state. (b) FLCE in bookshelf configuration. The polar axis is perpendicular to the film. Δd indicates the direction of the thickness change induced by a mechanical field [36]

two orientations of the polar axis are still possible due to different tilt directions of the smectic layers: the sample maintains macroscopically an apolar structure. A second shear deformation applied parallel to the smectic layer planes (see Fig. 17) finally leads to a polar sample [166, 167]. The influence of the second shear process on the polarity of the sample can be determined from the evolution of the piezoelectric constant d_{33} perpendicular to the tilt direction. Initially, areas with opposite polarity exist and the film does not show any signal, but if the mesogens become reoriented by the shear, a signal will be measured [168].

Starting materials for the preparation of FLCEs are depicted in Scheme 1. They include ferroelectric LC polymers with polymerizable groups (FLCE 1.1 and FLCE 2.2), which can be crosslinked as depicted in Fig. 3c; reactive ferroelectric monomer mixtures (FLCE 3.3, see Fig. 3d); and mesogens with vinyl groups that react with silanes to form either side-chain (FLCE 3.1 and BCFLCE) or main-chain polymers (FLCE 1.2) according to Fig. 3a. Although the first three examples (FLCE 1.1, FLCE 2.2, and FLCE 3.3) allow photocrosslinking in the neat s_C^* phase, FLCE 3.1 and BCFLCE require crosslinking in solution and thus a two-stage deformation process.

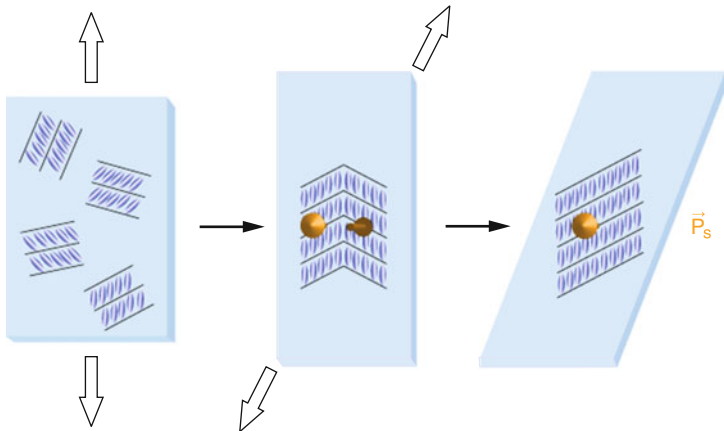


Fig. 17 Mechanical orientation of an FLCE by two stretching steps yields a polar monodomain [166, 167]. Depending on the procedure, the samples have a different thicknesses and director configurations

3.3 Electromechanical Properties of FLCEs

In this section we discuss the properties of FLCEs that are important for applications. Two options are possible: either a mechanical deformation generates a change of size or orientation of the polarization of the FLCE (an electric signal), or an applied electric field generates a deformation. In the case that an electric signal is detected, the piezoelectric constant is obtained. If the sample is deformed, the generated strain is of interest. Some characteristic values are collected in Table 1.

The first effect, piezoelectricity, is in principle well known for many types of polar materials [119]. The asymmetry of the switching observed for photocrosslinked elastomers (see Fig. 15) indicates stabilization of one particular switched state. This means that the sample must have a permanent dipole. If the sample is deformed, the director, and thereby the direction of the polar axis, changes. This effect is detected as an electric signal. Indeed a piezoelectric signal can be measured if the sample is deformed in the direction of the polar axis. As a consequence of the stabilization of the polar state, the sample shows a piezoelectric effect not only in the smectic-C* phase, but also in the smectic-A* phase [36]. The signal vanishes when the sample becomes isotropic (see Fig. 18).

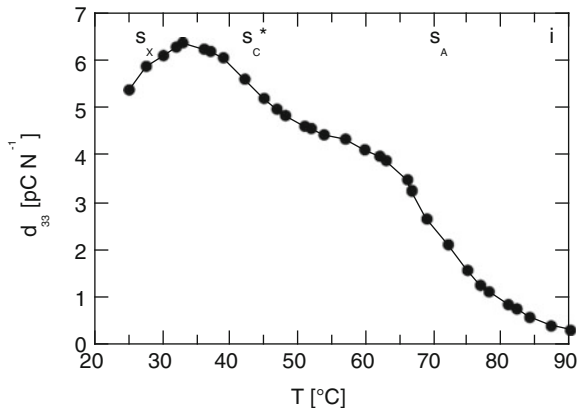
For the measurements presented in Fig. 18, the smectic-C* material FLCE1.1 (see Table 1), was crosslinked inside a commercial EHC glass cell with an electrode gap of 10 μm . Deformation of the cell with a force of 1 N induces a charge of 6 pC/cm^2 [36]. The magnitude of this value should be compared to the macroscopic spontaneous polarization P_s (macroscopic dipole moment) of the FLC under investigation. For the uncrosslinked FLC, P_s values of 40–60 nC/cm^2 have been observed [36]. Thus, if a full reversal of the orientation of P_s could be induced by

Table 1 Properties of different piezoelectric materials

Material	Group	Thickness (mm)	Elastic modulus (Pa)	Strain (%)	Piezoelectric coefficient (pC/N)	Electric field strength (V/ μ m)	Flexoelectric constant (nC/m)	Polarization (nC/cm ²)
PVDF	Goodfellow GmbH, Bad Nauheim, Germany	0.005	3.0×10^9	–	20	–	–	12×10^3
PZT	PI Ceramic GmbH, Lederhose, Germany	1.8	1.6×10^{11}	1.0×10^{-3}	150–300	–	–	14×10^3
FLCE1.1	ZenteI [36]	0.01	10×10^6	–	5	–	–	80
FLCE1.2	Kremer [168]	0.35	–	0.4	17.5	–	–	–
BCFLCE	Harden [169]	0.3	–	10	–	–	30	10
FLCE2.1	Kremer [170]	7.5×10^{-5}	10×10^6	3	–	1.5	–	80
FLCE2.2	Siannarius [171]	0.280	10×10^6	1	–	3	–	200
FLCE3.1	Hiraoka [172]	0.4	–	0.6	30	3	–	–
FLCE3.2	Ratna and Naciri [140]	0.06	–	5	–	13.3	–	–

PVDF polyvinylidene fluoride; PZT lead zirconium titanate; FLCE1 piezoelectric effect by compression perpendicular to the polar axis, planar alignment; FLCE2 electroclinic effect in homeotropic films; FLCE3 electroclinic effect in stretched film with planar alignment; BCFLCE flexoelectric effect on bent-core material

Fig. 18 Piezoelectric coefficient d_{33} of an FLCE crosslinked in the smectic- C^* phase. The stabilization of the polar order leads to a smectic- A^* phase that is also polar [36]



a mechanical deformation (elastic modulus of about 1 MPa [28–31, 173]), a piezo-response of similar magnitude would be expected. The observed value of a few pC/cm² is about a factor 10,000 smaller. The EHC cell is glued on the sides and some stress is taken up by the deformation of the cell alone. Thus, the resulting piezoelectric coefficient should be somewhat larger if the glass plates are not connected with each other. This has been seen for free-standing films of FLCE1.2 that show a value of 17.5 pC/N [168]. This value is, however, still much smaller than the spontaneous polarization. Obviously, a reorientation of the polar axis could not be achieved, because a mechanical deformation parallel to the polar axis is not very effective at rotating P_s . Shear deformations might be more useful.

To optimize the piezoelectric response, some studies on the structure–property relations are adequate. One would like to work with FLCEs with a strong coupling between the polar axis and the network. Thus ferroelectric main-chain polymers might be attractive (see Fig. 2). However, up to now, there have been only a few reports about ferroelectric switching in main-chain polymers [174–176] and none about switching the corresponding elastomers. Concerning LC side-chain polymers, the position of the netpoints is essential for determining the coupling between the polar axis (and thus the director) and the polymer network. In the experiments described above, the crosslinkable group was attached to the end of the mesogen. This means that the netpoints link the polymer chains via the mesogenic groups [36]. As the mesogens have to move during switching, this is a serious obstacle and long switching times of 1 s are measured at fields up to 500 V. This can be circumvented if the polymer chains are directly attached to each other without including mesogenic units. This leads to much faster switchable ferroelectric polymer networks [37, 177]. In that case, the coupling between polar axis and polymer network is rather weak and the piezoelectric effect should be low.

On an absolute scale, a comparison of FLCEs with crystalline (or semicrystalline) materials like polyvinylidene fluoride (PVDF) and ceramic materials like lead zirconium titanate (PZT) is necessary. These have much larger polarizations (see Table 1). However, their elastic modulus is also much higher (in the gigapascal range).

Accordingly, the piezoelectric coefficients measured for FLCEs and for other ferroelectric materials have a similar magnitude because for similar forces the elastomers are deformed more strongly.

Concerning the shape variations resulting from the application of an external electric field, the consequences of an induced ferroelectric switching will be discussed at first. As evident from Fig. 14a, both polar states are very similar and the deformation resulting from the rotation of the director on the cone can be considered to be rather small. In fact some “vibrations” have been observed during rapid switching of low-molar-mass ferroelectrics; thus the shape variations must be rather small [178, 179]. The electroclinic effect, on the other hand, promises much larger deformations (see Fig. 14b) and most experiments have focused in this direction. In free-standing films, the smectic layers are parallel to the film surface and the polar axis lies in the plane of the film. This arrangement is ideal for observation of the electroclinic effect around the smectic-A* to chiral smectic-C* phase transition (see Fig. 19a). If an electric field is applied parallel to the smectic layers, the chiral mesogens will tilt such that the induced polarity is opposite to the electric field. The tilt of the molecules is accompanied by a decrease in the smectic layer thickness. Due to the stacking of the smectic layers in the film, the thickness variation of the various layers is expected to add up and a reasonable change of the film thickness should be observed.

These considerations have led to several attempts to measure the thickness change of films in dependence on an applied electric field. In a first experiment, a Michelson interferometer was used for the determination of the thickness change in a 75-nm thick free-standing smectic film of FLCE2.1 (Scheme 1). With this method, a strain of 4% at a field of 1.5 V/ μm was measured [170], which would correspond to $a = 55 \times 10^{-15} \text{ m}^2/\text{V}^2$. In a second experiment (with the similar material FLCE2.2) reflection microscopy was used. This allowed simultaneous measurement of the decrease in film thickness and the associated increase in width of the sample (Fig. 20). In this experiment, a strain of only 1% was detected at a field of 3 V/ μm [171], corresponding to $a = 1 \times 10^{-15} \text{ m}^2/\text{V}^2$. Most probably the smaller value is correct [171], because its magnitude is consistent with tilt angle susceptibilities of similar materials [23, 25], for which induced tilt angles of the

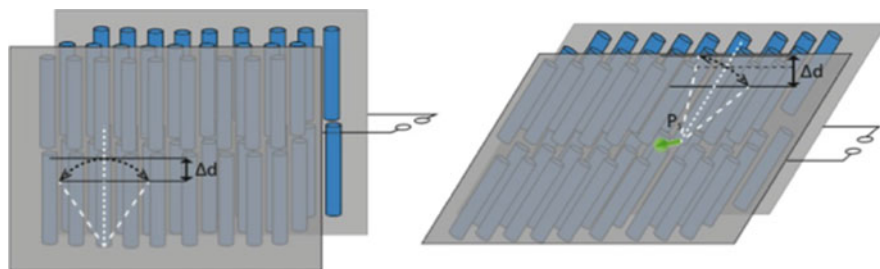
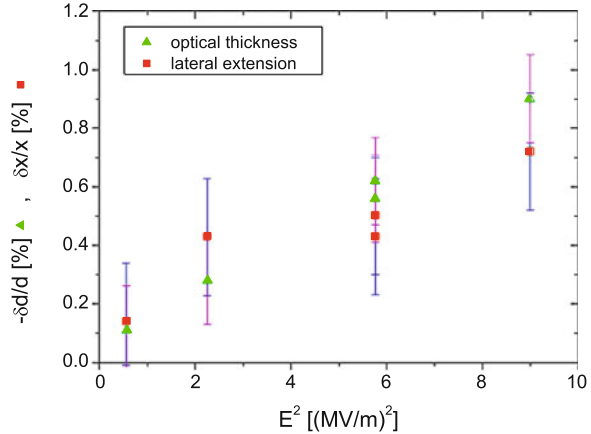


Fig. 19 (a) FLCE film crosslinked in the smectic-C* phase. (b) FLCE film crosslinked in the smectic-A* phase

Fig. 20 Change of sample width and thickness, respectively, during electroclinic switching of a free-standing FLCE film [171]



order of 5° are found for comparable electric fields. This explanation is also supported by the findings of other groups (see Table 1) that also give values in the range of $a = 1 \times 10^{-15} \text{ m}^2/\text{V}^2$. Independent of the exact magnitude of the shape variation accessible with free-standing films, these results belong to the highest values ever reported for piezoelectric materials. Possibly, the shape variation can be increased further using LCEs from main-chain polymers [174], but so far no such measurements have been reported.

Elastomer films oriented by the two-stage stretching process have been used for similar experiments. If the electroclinic effect is measured in such films, it should be realized that the smectic layers are now perpendicular to the film surface. Thus tilting of the mesogens, either by a phase transition or by an electric field, will be seen primarily by a change in the length of the film while the thickness will vary only slightly to conserve the volume. The two-step stretching gives a rhomboedric sample with ferroelectric monodomains (see Fig. 19) if the sample is crosslinked in the s_C^* phase. If such a sample is heated from the smectic- C^* to the smectic- A^* phase, the tilt angle approaches 0° . As a consequence of the crosslinking, a freely movable sample shows a macroscopic shear deformation during which it becomes rectangular and the length increases [138]. In this case, the macroscopic shape reflects the molecular arrangement: the mesogens change their orientation from tilted to perpendicular. With electrodes mounted to the film surface, the electroclinic effect can be observed in the smectic- C^* and the smectic- A^* phase. In the case of an elastomer crosslinked in the smectic- C^* phase (FLCE3.1, see Fig. 19) [180], the mesogens are tilted toward the layer normal. Upon application of an alternating current field the sample extends or shrinks depending on the polarity of the applied field. In one case, the electroclinic effect adds an additional tilt to the existing tilt and the sample shrinks. In the other situation, the electroclinic effect counteracts the tilt of the s_C^* phase and the sample becomes more elongated. If the elastomer sample is, however, crosslinked in the smectic- A^* phase (FLCE3.2) [140], the mesogens are oriented perpendicular to the smectic layers. After the application of an electric field, a tilt is induced and the film shrinks perpendicular to

the layers. This effect is independent of the polarity (tilting to the left or the right). The shrinking rate perpendicular to the smectic layers is comparable to the shrinking of the homeotropic film mentioned before. As described for the thermal transition, the thickness change that is caused by the electroclinic switching is always accompanied by shear parallel to the smectic layers.

So far we have discussed networks containing calamitic rod-like mesogens. Due to their kinked shape, bent-core LCs (BCLCs) also have ferroelectric properties. Though they have been known for about 15 years, because of their high phase transition temperatures it is hard to obtain oriented samples. As a consequence, low-molar-mass BCLC systems have mainly been investigated so far. In a first experiment, direct measurement of the flexoelectric effect was performed [112]. The mechanical deformation resulted in induced currents of up to 8 nA (at 5 Hz and a 4.8 cm² electrode area). This corresponds to a bend flexoelectric coefficient e_3 of 60 nC/m. In nonaligned samples, smaller values are observed that increase upon mechanical treatment. This is attributed to improvement of the degree of orientational order. In the case of smectic BCLCs, the behavior is even more complicated. These phases are primarily composed of alternating layers that prevent a macroscopic polar orientation. Such samples have to be poled to align the polar axis and to obtain a piezoelectric signal. After poling, a piezoelectric current of up to 20 nA (2 cm² sample area) has been measured [181]. This corresponds to a piezoelectric constant of 100 pC/N, a value comparable to PVDF and ceramic materials. However, due to a thermal back-relaxation to the macroscopically apolar state, this value cannot be maintained. At 60°C the half-life time of the measured current is only 50 s.

Crosslinking can be used to overcome the aforementioned obstacles, as in the case of the calamitic networks in which the orientation and polarity are preserved. First experiments were performed by swelling a calamitic LCE with a low-molar-mass BCLC [182, 183]. Up to 35 mol% of this material could be incorporated into the network. The resulting gel had a flexoelectric constant e_3 of 20 nC/m. This is one-third of the value of the low-molar-mass BCLC, which corresponds to the volume fraction of the BCLC. Only recently has a pure bent-core elastomer (BCFLCE) been made [139, 169]. Following the synthetic route of Finkelmann, an oriented, transparent nematic elastomer sample could be obtained. As a polysiloxane backbone was used, the T_g was close to room temperature. The flexoelectric constant of 40 nC/m is somewhat smaller than for the pure bend-core monomer, but larger than the value obtained for the swollen elastomer.

4 Conclusions and Outlook

LCEs have been under investigation for several years. These systems are unique because of the combination of order and softness. During recent years, several developments have evolved that bring them closer to application. One important achievement is the introduction of various stimuli like electric current and

irradiation with light that can, in addition to heat, trigger the NI phase transition and thereby the actuation process. In addition, FLCEs have been made that can produce a movement in an electric field without any phase transition. These new stimuli allow direct addressing of the actuator without the need to heat the whole device.

As far as synthesis is concerned, photochemistry has become the method of choice for crosslinking reactions. In this way, polymerization and crosslinking of monomeric liquid crystals can be initiated, as well as crosslinking of functional pre-polymers on demand. This allows the utilization on LCEs of several orientation techniques known from low-molar-mass liquid crystals, like electric fields and surface forces. Macroscopic machines have been constructed that use either the bending motion or the lateral deformation of an LCE actuator. Among them are locomotion devices that work both on land and in water, grippers, and devices that transform light into rotational energy.

The most important development in LCE research is miniaturization. Novel preparation techniques like lithography, inkjet printing, microfluidics, and electrospinning allow fabrication of aligned LCE samples on micrometer and even nanometer scales.

These advances are the most promising for use in real-world applications, because actuation on these scales is difficult to achieve with traditional methods. Potential applications are stimuli-responsive surfaces, microlenses, propulsion systems for microrobots, and lab-on-a-chip systems. In our opinion, future research in the field of LCEs will focus on these small scales.

References

1. Brand HR, Finkelmann H (1998) Physical properties of liquid crystalline elastomers. In: Demus D, Boodby J, Gray GW, Spiess HW (eds) Handbook of liquid crystals, vol. 3, Chap. 5. Wiley-VCH, Weinheim. doi:[10.1002/9783527620593.ch5](https://doi.org/10.1002/9783527620593.ch5)
2. Brand HR, Pleiner H, Martinoty P (2006) Selected macroscopic properties of liquid crystalline elastomers. *Soft Matter* 2(3):182–189. doi:[10.1039/b512693m](https://doi.org/10.1039/b512693m)
3. Brehmer M, Zentel R (1994) Liquid crystalline elastomers- characterization as networks. *Mol Cryst Liq Cryst Sci Technol Sect A-Mol Cryst Liq Cryst* 243:353–376. doi:[10.1080/10587259408037775](https://doi.org/10.1080/10587259408037775)
4. Finkelmann H, Brand HR (1994) Liquid crystalline elastomers - a class of materials with novel properties. *Trends Polym Sci* 2 (7):222–226
5. Ohm C, Brehmer M, Zentel R (2010) Liquid crystalline elastomers as actuators and sensors. *Adv Mater* 22(31):3366–3387. doi:[10.1002/Adma.200904059](https://doi.org/10.1002/Adma.200904059)
6. Terentjev EM (1999) Liquid-crystalline elastomers. *J Phys-Condens Matter* 11(24):R239–R257. doi:[10.1088/0953-8984/11/24/201](https://doi.org/10.1088/0953-8984/11/24/201)
7. Urayama K (2007) Selected issues in liquid crystal elastomers and gels. *Macromolecules* 40 (7):2277–2288. doi:[10.1021/ma0623688](https://doi.org/10.1021/ma0623688)
8. Warner M, Terentjev EM (2003) Liquid crystal elastomers, vol 120. International series of monographs on physics. Oxford University Press, Oxford. doi:<http://ukcatalogue.oup.com/product/9780198527671.doa>
9. Xie P, Zhang RB (2005) Liquid crystal elastomers, networks and gels: advanced smart materials. *J Mater Chem* 15(26):2529–2550. doi:[10.1039/b413835j](https://doi.org/10.1039/b413835j)

10. Zentel R (1989) Liquid crystalline elastomers. *Angew Chem Int Ed Engl* 28(10):1407–1415
11. de Gennes PG (1975) One type of nematic polymers. *Comptes Rendus Hebdomadaires Des Seances De L Academie Des Sciences Serie B* 281(5–8):101–103
12. de Gennes PG, Hebert M, Kant R (1996) Artificial muscles based on nematic gels. In: 2nd international symposium on molecular order and mobility in polymer systems, St Petersburg, Russia, 21–24 May 1996. Huthig & Wepf Verlag, pp 39–49. doi:[10.1002/masy.19971130107](https://doi.org/10.1002/masy.19971130107)
13. Mirfakhrai T, Madden JDW, Baughman RH (2007) Polymer artificial muscles. *Mater Today* 10(4):30–38. doi:[10.1016/S1369-7021\(07\)70048-2](https://doi.org/10.1016/S1369-7021(07)70048-2)
14. Selinger RLB, Mbanga BL, Selinger JV (2008) Modeling liquid crystal elastomers: actuators, pumps, and robots – art. no. 69110A. In: Chien LC (ed) Conference on emerging liquid crystal technologies III, San Jose, CA, 20–22 Jan 2008. SPIE-int soc optical engineering, p A9110. doi:[10.1117/12.768282](https://doi.org/10.1117/12.768282)
15. Madden JDW, Vandesteeg NA, Anquetil PA, Madden PGA, Takshi A, Pytel RZ, Lafontaine SR, Wieringa PA, Hunter IW (2003) Artificial muscle technology: physical principles and naval prospects. In: 13th international symposium on unmanned untethered submersible technology, Durham, NH, 24–27 Aug 2003. IEEE-Inst Electrical Electronics Engineers Inc, pp 706–728. doi:[10.1109/joe.2004.833135](https://doi.org/10.1109/joe.2004.833135)
16. Yang H, Buguin A, Taulemesse J-M, Kaneko K, Méry S, Bergeret A, Keller P (2009) Micron-sized main-chain liquid crystalline elastomer actuators with ultralarge amplitude contractions. *J Am Chem Soc* 131(41):15000–15004. doi:[10.1021/ja905363f](https://doi.org/10.1021/ja905363f)
17. Bualek S, Kapitza H, Meyer J, Schmidt GF, Zentel R (1988) Orientability of crosslinked and of chiral liquid-crystalline polymers. *Mol Cryst Liq Cryst* 155:47–56. doi:[10.1080/00268948808070351](https://doi.org/10.1080/00268948808070351)
18. Küpfer J, Finkelmann H (1991) Nematic liquid single-crystal elastomers. *Makromol Chem-Rapid Commun* 12(12):717–726. doi:[10.1002/marc.1991.030121211](https://doi.org/10.1002/marc.1991.030121211)
19. Öge T, Zentel R (1996) Manipulation of the ferroelectricity in LC polymers via photomechanical isomerization of azobenzene moieties. *Macromol Chem Phys* 197(6):1805–1813
20. de Jeu WH (1980) Physical properties of liquid crystalline materials, vol 1, Liquid crystal monographs. Gordon and Breach, New York
21. Kempe MD, Scruggs NR, Verduzco R, Lal J, Kornfield JA (2004) Self-assembled liquid-crystalline gels designed from the bottom up. *Nat Mater* 3(3):177–182. doi:[10.1038/nmat1074](https://doi.org/10.1038/nmat1074)
22. Li JJ, Stannarius R, Tolksdorf C, Zentel R (2003) Hydrogen bonded ferroelectric liquid crystal gels in freely suspended film geometry. *Phys Chem Chem Phys* 5(5):916–923. doi:[10.1039/b205210e](https://doi.org/10.1039/b205210e)
23. Brehmer M, Zentel R, Giesselmann F, Germer R, Zugenmaier P (1996) Coupling of liquid crystalline and polymer network properties in LC-elastomers. *Liq Cryst* 21(4):589–596. doi:[10.1080/02678299608032868](https://doi.org/10.1080/02678299608032868)
24. Garoff S, Meyer RB (1977) Electro-clinic effect at A/C phase-change in a chiral smectic liquid-crystal. *Phys Rev Lett* 38(15):848–851. doi:[10.1103/PhysRevLett.38.848](https://doi.org/10.1103/PhysRevLett.38.848)
25. Poths H, Andersson G, Skarp K, Zentel R (1992) Fast electroclinic switching in a ferroelectric LC-polysiloxane. *Adv Mater* 4(12):792–794. doi:[10.1002/adma.19920041204](https://doi.org/10.1002/adma.19920041204)
26. Finkelmann H, Ringsdorf H, Wendorff JH (1978) Model considerations and examples of enantiotropic liquid-crystalline polymers - polyreactions in ordered systems, 14. *Makromol Chem - Macromol Chem Phys* 179(1):273–276. doi:[10.1002/macp.1978.021790129](https://doi.org/10.1002/macp.1978.021790129)
27. Zentel R (1994) Liquid crystalline polymers. In: Stegemeyer H (ed) Liquid crystals. Steinkopff, Darmstadt, pp 103–140
28. Kaufhold W, Finkelmann H, Brand HR (1991) Nematic elastomers. 1. Effect of the spacer length on the mechanical coupling between network anisotropy and nematic order. *Makromol Chem - Macromol Chem Phys* 192(11):2555–2579. doi:[10.1002/macp.1991.021921104](https://doi.org/10.1002/macp.1991.021921104)
29. Martinoty P, Stein P, Finkelmann H, Pleiner H, Brand HR (2004) Mechanical properties of monodomain side chain nematic elastomers. *Eur Phys J E* 14(4):311–321. doi:[10.1140/epje/i2003-10154-y](https://doi.org/10.1140/epje/i2003-10154-y)

30. Pakula T, Zentel R (1991) Mechanical behavior of liquid-crystalline side-group polymers and their networks. *Makromol Chem - Macromol Chem Phys* 192(10):2401–2410. doi:[10.1002/macp.1991.021921018](https://doi.org/10.1002/macp.1991.021921018)
31. Zentel R, Wu JS (1986) Rheological properties of liquid crystalline side-group polymers in the isotropic, nematic and smectic states. *Makromol Chem - Macromol Chem Phys* 187(7): 1727–1736. doi:[10.1002/macp.1986.021870716](https://doi.org/10.1002/macp.1986.021870716)
32. Hikmet RAM, Lub J, Broer DJ (1991) Anisotropic networks formed by photopolymerization of liquid-crystalline molecules. *Adv Mater* 3(7–8):392–394. doi:[10.1002/adma.19910030713](https://doi.org/10.1002/adma.19910030713)
33. Li MH, Keller P, Yang JY, Albouy PA (2004) An artificial muscle with lamellar structure based on a nematic triblock copolymer. *Adv Mater* 16(21):1922–1925. doi:[10.1002/adma.200400658](https://doi.org/10.1002/adma.200400658)
34. Wiesemann A, Zentel R, Pakula T (1992) Redox-active liquid-crystalline ionomers.1. Synthesis and rheology. *Polymer* 33(24):5315–5320. doi:[10.1016/0032-3861\(92\)90818-H](https://doi.org/10.1016/0032-3861(92)90818-H)
35. Rogez D, Martinoty P (2011) Mechanical properties of monodomain nematic side-chain liquid-crystalline elastomers with homeotropic and in-plane orientation of the director. *Eur Phys J E Soft matter* 34(7):69. doi:[10.1140/epje/i2011-11069-8](https://doi.org/10.1140/epje/i2011-11069-8)
36. Brehmer M, Zentel R, Wagenblast G, Siemensmeyer K (1994) Ferroelectric liquid crystalline elastomers. *Macromol Chem Phys* 195(6):1891–1904. doi:[10.1002/macp.1994.021950601](https://doi.org/10.1002/macp.1994.021950601)
37. Gebhard E, Zentel R (2000) Ferroelectric liquid crystalline elastomers, 1 - Variation of network topology and orientation. *Macromol Chem Phys* 201(8):902–910. doi:[10.1002/\(SICI\)1521-3935\(20000501\)201:8<902::AID-MACP902>3.0.CO;2-9](https://doi.org/10.1002/(SICI)1521-3935(20000501)201:8<902::AID-MACP902>3.0.CO;2-9)
38. Gebhard E, Zentel R (2000) Ferroelectric liquid crystalline elastomers, 2 - Variation of mesogens and network density. *Macromol Chem Phys* 201(8):911–922. doi:[10.1002/\(SICI\)1521-3935\(20000501\)201:8<911::AID-MACP911>3.0.CO;2-9](https://doi.org/10.1002/(SICI)1521-3935(20000501)201:8<911::AID-MACP911>3.0.CO;2-9)
39. Kapitza H, Zentel R (1991) Chiral liquid-crystalline elastomers by polymer-analogous reactions. *Makromol Chem - Macromol Chem Phys* 192(8):1859–1872. doi:[10.1002/macp.1991.021920821](https://doi.org/10.1002/macp.1991.021920821)
40. Ikeda T, Nakano M, Yu YL, Tsutsumi O, Kanazawa A (2003) Anisotropic bending and unbending behavior of azobenzene liquid-crystalline gels by light exposure. *Adv Mater* 15(3):201–205. doi:[10.1002/adma.200390045](https://doi.org/10.1002/adma.200390045)
41. Beyer P, Braun L, Zentel R (2007) (Photo)crosslinkable smectic LC main-chain polymers. *Macromol Chem Phys* 208(22):2439–2448. doi:[10.1002/macp.200700292](https://doi.org/10.1002/macp.200700292)
42. Beyer P, Terentjev EM, Zentel R (2007) Monodomain liquid crystal main chain elastomers by photocrosslinking. *Macromol Rapid Commun* 28(14):1485–1490. doi:[10.1002/marc.200700210](https://doi.org/10.1002/marc.200700210)
43. Komp A, Ruhe J, Finkelmann H (2005) A versatile preparation route for thin free-standing liquid single crystal elastomers. *Macromol Rapid Commun* 26(10):813–818. doi:[10.1002/marc.200500049](https://doi.org/10.1002/marc.200500049)
44. McKenzie BM, Wojtecki RJ, Burke KA, Zhang C, Jakli A, Mather PT, Rowan SJ (2011) Metallo-responsive liquid crystalline monomers and polymers. *Chem Mater* 23(15): 3525–3533. doi:[10.1021/cm2011617](https://doi.org/10.1021/cm2011617)
45. Fox JD, Rowan SJ (2009) Supramolecular polymerizations and main-chain supramolecular polymers. *Macromolecules* 42(18):6823–6835. doi:[10.1021/ma901144t](https://doi.org/10.1021/ma901144t)
46. Oriol L, Pinol M, Serrano JL (1997) The state of the art in metallomesogenic polymers. *Prog Polym Sci* 22(5):873–911. doi:[10.1016/s0079-6700\(97\)00011-7](https://doi.org/10.1016/s0079-6700(97)00011-7)
47. Ahir SV, Tajbakhsh AR, Terentjev EM (2006) Self-assembled shape-memory fibers of triblock liquid-crystal polymers. *Adv Funct Mater* 16(4):556–560. doi:[10.1002/adfm.200500692](https://doi.org/10.1002/adfm.200500692)
48. Finkelmann H (1987) Liquid crystalline polymers. *Angew Chem Int Ed Engl* 26(9):816–824. doi:[10.1002/anie.198708161](https://doi.org/10.1002/anie.198708161)
49. Boeffel C, Spiess HW, Hisgen B, Ringsdorf H, Ohm H, Kirste RG (1986) Molecular order of spacer and main chain in polymeric side-group liquid-crystals. *Makromol Chem Rapid Commun* 7(12):777–783

50. Noirez L, Keller P, Cotton JP (1995) On the structure and the chain conformation of side-chain liquid-crystal polymers. *Liq Cryst* 18(1):129–148. doi:[10.1080/02678299508036602](https://doi.org/10.1080/02678299508036602)
51. Leroux N, Keller P, Achard MF, Noirez L, Hardouin F (1993) Small-angle neutron-scattering experiments on side-on fixed liquid-crystal polyacrylates. *J Phys II* 3(8):1289–1296. doi:[10.1051/jp2:1993199](https://doi.org/10.1051/jp2:1993199)
52. Arrighi V, Higgins JS, Weiss RA, Cimecioglu AL (1992) A small-angle neutron scattering study of a semi-flexible main-chain liquid-crystalline copolyester. *Macromolecules* 25(20):5297–5305
53. Dallest JF, Maissa P, Tenbosch A, Sixou P, Blumstein A, Blumstein R, Teixeira J, Noirez L (1988) Experimental evidence of chain extension at the transition-temperature of a nematic polymer. *Phys Rev Lett* 61(22):2562–2565. doi:[10.1103/PhysRevLett.61.2562](https://doi.org/10.1103/PhysRevLett.61.2562)
54. Hardouin F, Leroux N, Méry S, Noirez L (1992) Small-angle neutron-scattering experiments on side-on fixed liquid-crystal polysiloxanes. *J Phys II* 2(3):271–278. doi:[10.1051/jp2:1992131](https://doi.org/10.1051/jp2:1992131)
55. Keller P, Carvalho B, Cotton JP, Lambert M, Moussa F, Pepy G (1985) Side-chain mesomorphic polymers—studies labeled backbones by neutron-scattering. *Journal De Physique Lettres* 46(22):1065–1071. doi:[10.1051/jphyslet:0198500460220106500](https://doi.org/10.1051/jphyslet:0198500460220106500)
56. Kirste RG, Ohm HG (1985) The conformation of liquid-crystalline polymers as revealed by neutron-scattering. *Makromol Chem Rapid Commun* 6(3):179–185. doi:[10.1002/marc.1985.030060312](https://doi.org/10.1002/marc.1985.030060312)
57. Ohm HG, Kirste RG, Oberthur RC (1988) The backbone conformation of liquid-crystalline side-chain polymers in the mesophases and in the isotropic phase determined by scattering methods. *Makromol Chem Macromol Chem Phys* 189(6):1387–1405. doi:[10.1002/macp.1988.021890616](https://doi.org/10.1002/macp.1988.021890616)
58. Pepy G, Noirez L, Keller P, Lambert M, Moussa F, Cotton JP, Strazielle C, Lapp A, Hardouin F, Mauzac M, Richard H (1990) Observation of the conformation and structure of some liquid-crystal polymers by small-angle neutron-scattering. *Makromol Chem Macromol Chem Phys* 191(6):1383–1392. doi:[10.1002/macp.1990.021910617](https://doi.org/10.1002/macp.1990.021910617)
59. Thomsen DL, Keller P, Naciri J, Pink R, Jeon H, Shenoy D, Ratna BR (2001) Liquid crystal elastomers with mechanical properties of a muscle. *Macromolecules* 34(17):5868–5875. doi:[10.1021/ma001639q](https://doi.org/10.1021/ma001639q)
60. Wermter H, Finkelmann H (2001) Liquid crystalline elastomers as artificial muscles. *e-Polymers* 013. Available at http://www.e-polymers.org/journal/papers/finkelmann_210801.pdf
61. Tajbakhsh AR, Terentjev EM (2001) Spontaneous thermal expansion of nematic elastomers. *Eur Phys J E* 6(2):181–188. doi:[10.1007/s101890170020](https://doi.org/10.1007/s101890170020)
62. Beyer P, Krueger M, Giesselmann F, Zentel R (2007) Photoresponsive ferroelectric liquid-crystalline polymers. *Adv Funct Mater* 17(1):109–114. doi:[10.1002/Adfm.200600513](https://doi.org/10.1002/Adfm.200600513)
63. Komp A, Finkelmann H (2007) A new type of macroscopically oriented smectic-A liquid crystal elastomer. *Macromol Rapid Commun* 28(1):55–62. doi:[10.1002/marc.200600640](https://doi.org/10.1002/marc.200600640)
64. Nishikawa E, Finkelmann H (1999) Smectic-A liquid single crystal elastomers – strain induced break-down of smectic layers. *Macromol Chem Phys* 200(2):312–322. doi:[10.1002/\(SICI\)1521-3935\(19990201\)200:2<312::AID-MACP312>3.0.CO;2-Y](https://doi.org/10.1002/(SICI)1521-3935(19990201)200:2<312::AID-MACP312>3.0.CO;2-Y)
65. Sanchez-Ferrer A, Finkelmann H (2009) Thermal and mechanical properties of new main-chain liquid-crystalline elastomers. *Mol Cryst Liq Cryst* 508:348–356. doi:[10.1080/15421400903065861](https://doi.org/10.1080/15421400903065861)
66. Poths H, Zentel R (1994) Structure–property relationships of diluted ferroelectric polysiloxanes. *Liq Cryst* 16(5):749–767. doi:[10.1080/02678299408027848](https://doi.org/10.1080/02678299408027848)
67. Stannarius R, Schuring H, Tolksdorf C, Zentel R (2001) Elastic properties of liquid crystal elastomer balloons. *Mol Cryst Liq Cryst* 364:305–312. doi:[10.1080/10587250108024999](https://doi.org/10.1080/10587250108024999)
68. Ohm C, Morys M, Forst FR, Braun L, Eremin A, Serra C, Stannarius R, Zentel R (2011) Preparation of actuating fibres of oriented main-chain liquid crystalline elastomers by a wet spinning process. *Soft Matter* 7(8):3730–3734. doi:[10.1039/c1sm05111c](https://doi.org/10.1039/c1sm05111c)

69. Ohm C, Fleischmann EK, Kraus I, Serra C, Zentel R (2010) Control of the properties of micrometer-sized actuators from liquid crystalline elastomers prepared in a microfluidic setup. *Adv Funct Mater* 20(24):4314–4322. doi:[10.1002/adfm.201001178](https://doi.org/10.1002/adfm.201001178)
70. de Jeu WH, Obraztsov EP, Ostrovskii BI, Ren W, McMullan PJ, Griffin AC, Sanchez-Ferrer A, Finkelmann H (2007) Order and strain in main-chain smectic liquid-crystalline polymers and elastomers. *Eur Phys J E* 24(4):399–409. doi:[10.1140/epje/i2007-10254-8](https://doi.org/10.1140/epje/i2007-10254-8)
71. Demus D, Goodby J, Gray GW, Spiess HW (2008) Handbook of liquid crystals set. Wiley-VCH Verlag GmbH, Weinheim. doi:[10.1002/9783527619276](https://doi.org/10.1002/9783527619276)
72. Spillmann CA, Naciri J, Martin BD, Farahat W, Herr H, Ratna BR (2005) Stacking nematic elastomers for artificial muscle applications. In: 3rd international conference on materials for advanced technologies (ICMAT-2005)/9th international conference on advanced materials (ICAM 2005), Singapore, SINGAPORE, 03–08 July 2005. pp 500–505. doi:[10.1016/j.sna.2006.04.045](https://doi.org/10.1016/j.sna.2006.04.045)
73. Chambers M, Finkelmann H, Remskar M, Sanchez-Ferrer A, Zalar B, Zumer S (2009) Liquid crystal elastomer-nanoparticle systems for actuation. *J Mater Chem* 19(11):1524–1531. doi:[10.1039/b812423j](https://doi.org/10.1039/b812423j)
74. Yang LQ, Setyowati K, Li A, Gong SQ, Chen J (2008) Reversible infrared actuation of carbon nanotube-liquid crystalline elastomer nanocomposites. *Adv Mater* 20(12):2271–2275. doi:[10.1002/adma.200702953](https://doi.org/10.1002/adma.200702953)
75. Kaiser A, Winkler M, Krause S, Finkelmann H, Schmidt AM (2009) Magnetoactive liquid crystal elastomer nanocomposites. *J Mater Chem* 19(4):538–543. doi:[10.1039/b813120c](https://doi.org/10.1039/b813120c)
76. Ikeda T, Tsutsumi O (1995) Optical switching and image storage by means of azobenzene liquid-crystal films. *Science* 268(5219):1873–1875. doi:[10.1126/science.268.5219.1873](https://doi.org/10.1126/science.268.5219.1873)
77. Camacho-Lopez M, Finkelmann H, Palffy-Muhoray P, Shelley M (2004) Fast liquid-crystal elastomer swims into the dark. *Nat Mater* 3(5):307–310. doi:[10.1038/nmat1118](https://doi.org/10.1038/nmat1118)
78. Finkelmann H, Nishikawa E, Pereira GG, Warner M (2001) A new opto-mechanical effect in solids. *Phys Rev Lett* 87(1):4. doi:[01550110.1103/PhysRevLett.87.015501](https://doi.org/10.1103/PhysRevLett.87.015501)
79. Hogan PM, Tajbakhsh AR, Terentjev EM (2002) uv manipulation of order and macroscopic shape in nematic elastomers. *Phys Rev E* 65(4):10. doi:[04172010.1103/PhysRevE.65.041720](https://doi.org/10.1103/PhysRevE.65.041720)
80. Li MH, Keller P, Li B, Wang XG, Brunet M (2003) Light-driven side-on nematic elastomer actuators. *Adv Mater* 15(7–8):569–572. doi:[10.1002/adma.200304552](https://doi.org/10.1002/adma.200304552)
81. Yin RY, Xu WX, Kondo M, Yen CC, Mamiya J, Ikeda T, Yu YL (2009) Can sunlight drive the photoinduced bending of polymer films? *J Mater Chem* 19(20):3141–3143. doi:[10.1039/b904973h](https://doi.org/10.1039/b904973h)
82. van Oosten CL, Bastiaansen CWM, Broer DJ (2009) Printed artificial cilia from liquid-crystal network actuators modularly driven by light. *Nat Mater* 8(8):677–682. doi:[10.1038/nmat2487](https://doi.org/10.1038/nmat2487)
83. Yu YL, Nakano M, Ikeda T (2003) Directed bending of a polymer film by light – miniaturizing a simple photomechanical system could expand its range of applications. *Nature* 425(6954):145. doi:[10.1038/425145a](https://doi.org/10.1038/425145a)
84. Vennes M, Zentel R, Rossle M, Stepputat M, Kolb U (2005) Smectic liquid-crystalline colloids by miniemulsion techniques. *Adv Mater* 17(17):2123–2127. doi:[10.1002/adma.200500310](https://doi.org/10.1002/adma.200500310)
85. Haseloh S, van der Schoot P, Zentel R (2010) Control of mesogen configuration in colloids of liquid crystalline polymers. *Soft Matter* 6(17):4112–4119. doi:[10.1039/c0sm00125b](https://doi.org/10.1039/c0sm00125b)
86. Haseloh S, Ohm C, Smallwood F, Zentel R (2011) Nanosized shape-changing colloids from liquid crystalline elastomers. *Macromol Rapid Commun* 32(1):88–93
87. Ohm C, Kapernaum N, Nonnenmacher D, Giesselmann F, Serra C, Zentel R (2011) Microfluidic synthesis of highly shape-anisotropic particles from liquid crystalline elastomers with defined director field configurations. *J Am Chem Soc* 133(14):5305–5311. doi:[10.1021/ja1095254](https://doi.org/10.1021/ja1095254)
88. Yang H, Ye G, Wang XG, Keller P (2011) Micron-sized liquid crystalline elastomer actuators. *Soft Matter* 7(3):815–823. doi:[10.1039/c0sm00734j](https://doi.org/10.1039/c0sm00734j)

89. Zentel R, Strobl GR (1984) Structures of liquid crystalline side group polymers oriented by drawing. *Makromol Chem - Macromol Chem Phys* 185(12):2669–2676. doi:[10.1002/macp.1984.021851217](https://doi.org/10.1002/macp.1984.021851217)
90. Kim ST, Finkelmann H (2001) Cholesteric liquid single-crystal elastomers (LSCE) obtained by the anisotropic deswelling method. *Macromol Rapid Commun* 22(6):429–433. doi:[10.1002/1521-3927\(20010301\)22:6<429::AID-MARC429>3.0.CO;2-#](https://doi.org/10.1002/1521-3927(20010301)22:6<429::AID-MARC429>3.0.CO;2-#)
91. Nishikawa E, Yamamoto J, Yokoyama H, Finkelmann H (2004) Smectic a elastomers with uniform homeotropic orientation obtained by applying a biaxial mechanical field. *Macromol Rapid Commun* 25(5):611–617. doi:[10.1002/marc.200300183](https://doi.org/10.1002/marc.200300183)
92. Harris KD, Cuypers R, Scheibe P, van Oosten CL, Bastiaansen CWM, Lub J, Broer DJ (2005) Large amplitude light-induced motion in high elastic modulus polymer actuators. *J Mater Chem* 15(47):5043–5048. doi:[10.1039/b512655j](https://doi.org/10.1039/b512655j)
93. Elias AL, Harris KD, Bastiaansen CWM, Broer DJ, Brett MJ (2006) Photopatterned liquid crystalline polymers for microactuators. *J Mater Chem* 16(28):2903–2912. doi:[10.1039/b605511g](https://doi.org/10.1039/b605511g)
94. Yamada M, Kondo M, Mamiya JI, Yu YL, Kinoshita M, Barrett CJ, Ikeda T (2008) Photomobile polymer materials: towards light-driven plastic motors. *Angew Chem Int Ed* 47(27):4986–4988. doi:[10.1002/anie.200800760](https://doi.org/10.1002/anie.200800760)
95. Krause S, Dersch R, Wendorff JH, Finkelmann H (2007) Photocrosslinkable liquid crystal main-chain polymers: thin films and electrospinning. *Macromol Rapid Commun* 28(21):2062–2068. doi:[10.1002/marc.200700460](https://doi.org/10.1002/marc.200700460)
96. Odell JA, Keller A, Mueller AJ (1989) Extensional flow behavior of macromolecules in solution. In: *Polymers in aqueous media*, vol 223. *Advances in Chemistry*. American Chemical Society, Washington, pp 193–244. doi:[10.1021/ba-1989-0223.ch011](https://doi.org/10.1021/ba-1989-0223.ch011)
97. Naciri J, Srinivasan A, Jeon H, Nikolov N, Keller P, Ratna BR (2003) Nematic elastomer fiber actuator. *Macromolecules* 36(22):8499–8505. doi:[10.1021/ma034921g](https://doi.org/10.1021/ma034921g)
98. Ohm C, Serra C, Zentel R (2009) A continuous flow synthesis of micrometer-sized actuators from liquid crystalline elastomers. *Adv Mater* 21(47):4859–4862. doi:[10.1002/adma.200901522](https://doi.org/10.1002/adma.200901522)
99. Cairns DR, Shafran MS, Sierros KA, Huebsch WW, Kessrnan AJ (2010) Stimulus-responsive fluidic dispersions of rod shaped liquid crystal polymer colloids. *Mater Lett* 64(10):1133–1136. doi:[10.1016/j.matlet.2010.02.021](https://doi.org/10.1016/j.matlet.2010.02.021)
100. Ohm C, Haberkorn N, Theato P, Zentel R (2011) Template-based fabrication of nanometer-scaled actuators from liquid-crystalline elastomers. *Small* 7(2):194–198. doi:[10.1002/sml.201001315](https://doi.org/10.1002/sml.201001315)
101. Yang ZQ, Huck WTS, Clarke SM, Tajbakhsh AR, Terentjev EM (2005) Shape-memory nanoparticles from inherently non-spherical polymer colloids. *Nat Mater* 4(6):486–490. doi:[10.1038/nmat1389](https://doi.org/10.1038/nmat1389)
102. Ikeda T, Mamiya J, Yu YL (2007) Photomechanics of liquid-crystalline elastomers and other polymers. *Angew Chem Int Ed* 46(4):506–528. doi:[10.1002/anie.200602372](https://doi.org/10.1002/anie.200602372)
103. Yamada M, Kondo M, Miyasato R, Naka Y, Mamiya J, Kinoshita M, Shishido A, Yu YL, Barrett CJ, Ikeda T (2009) Photomobile polymer materials-various three-dimensional movements. *J Mater Chem* 19(1):60–62. doi:[10.1039/b815289f](https://doi.org/10.1039/b815289f)
104. White TJ, Serak SV, Tabiryan NV, Vaia RA, Bunning TJ (2009) Polarization-controlled, photodriven bending in monodomain liquid crystal elastomer cantilevers. *J Mater Chem* 19(8):1080–1085. doi:[10.1039/b818457g](https://doi.org/10.1039/b818457g)
105. Anderle K, Birenheide R, Werner MJA, Wendorff JH (1991) Molecular addressing - studies on light-induced reorientation in liquid-crystalline side-chain polymers. *Liq Cryst* 9(5):691–699. doi:[10.1080/02678299108030382](https://doi.org/10.1080/02678299108030382)
106. Natansohn A, Rochon P, Gosselin J, Xie S (1992) Azo polymers for reversible optical storage. 1. poly[4'-[[2-(acryloyloxy)ethyl]ethylamino]-4-nitroazobenzene]. *Macromolecules* 25(8):2268–2273. doi:[10.1021/ma00034a031](https://doi.org/10.1021/ma00034a031)

107. Sanchez-Ferrer A, Fischl T, Stubenrauch M, Wurmus H, Hoffmann M, Finkelmann H (2009) Photo-crosslinked side-chain liquid-crystalline elastomers for microsystems. *Macromol Chem Phys* 210(20):1671–1677. doi:[10.1002/macp.200900308](https://doi.org/10.1002/macp.200900308)
108. Sungur E, Li MH, Taupier G, Boeglin A, Romeo M, Mery S, Keller P, Dorkenoo KD (2007) External stimulus driven variable-step grating in a nematic elastomer. *Opt Express* 15(11): 6784–6789
109. Sungur E, Mager L, Boeglin A, Li MH, Keller P, Dorkenoo KD (2010) Temperature tunable optical gratings in nematic elastomer. *Appl Phys A Mater Sci Process* 98(1):119–122. doi:[10.1007/s00339-009-5448-z](https://doi.org/10.1007/s00339-009-5448-z)
110. Harris KD, Bastiaansen CWM, Lub J, Broer DJ (2005) Self-assembled polymer films for controlled agent-driven motion. *Nano Lett* 5(9):1857–1860. doi:[10.1021/nl0514590](https://doi.org/10.1021/nl0514590)
111. Clark NA, Lagerwall ST (1980) Submicrosecond bistable electro-optic switching in liquid-crystals. *Appl Phys Lett* 36(11):899–901. doi:[10.1063/1.91359](https://doi.org/10.1063/1.91359)
112. Harden J, Mbangi B, Eber N, Fodor-Csorba K, Sprunt S, Gleeson JT, Jakli A (2006) Giant flexoelectricity of bent-core nematic liquid crystals. *Phys Rev Lett* 97. doi:[10.1103/PhysRevLett.97.157802](https://doi.org/10.1103/PhysRevLett.97.157802)
113. Lagerwall ST (2007) The necessary conditions for macroscopic polarization. In: *Ferroelectric and antiferroelectric liquid crystals*. Wiley-VCH Verlag GmbH, Weinheim, pp 57–91. doi:[10.1002/9783527613588.ch3](https://doi.org/10.1002/9783527613588.ch3)
114. Ho RM, Chiang YW, Lin SC, Chen CK (2011) Helical architectures from self-assembly of chiral polymers and block copolymers. *Prog Polym Sci* 36(3):376–453. doi:[10.1016/j.progpolymsci.2010.09.001](https://doi.org/10.1016/j.progpolymsci.2010.09.001)
115. Brochu P, Pei QB (2010) Advances in dielectric elastomers for actuators and artificial muscles. *Macromol Rapid Commun* 31(1):10–36. doi:[10.1002/marc.200900425](https://doi.org/10.1002/marc.200900425)
116. Lagerwall JPF, Giesselmann F (2006) Current topics in smectic liquid crystal research. *ChemPhysChem* 7(1):20–45. doi:[10.1002/cphc.200500472](https://doi.org/10.1002/cphc.200500472)
117. Zentel R, Gebhard E, Brehmer M (2000) Ferroelectric LC-elastomers. *Adv Chem Phys* 113:159–182. doi:[10.1002/9780470141724.ch4](https://doi.org/10.1002/9780470141724.ch4)
118. Kremer F, Skupin H, Lehmann W, Hartmann L, Stein P, Finkelmann H (2000) Structure, mobility, and piezoelectricity in ferroelectric liquid crystalline elastomers. *Adv Chem Phys* 113:183–201. doi:[10.1002/9780470141724.ch5](https://doi.org/10.1002/9780470141724.ch5)
119. Brehmer M, Zentel R (2011) Ferroelectric liquid crystalline elastomers. In: *Encyclopedia of polymer science and technology*. Wiley. doi:[10.1002/0471440264.pst429.pub2](https://doi.org/10.1002/0471440264.pst429.pub2)
120. Walba DM, Xiao L, Keller P, Shao RF, Link D, Clark NA (1999) Ferroelectric liquid crystals for second order nonlinear optics. *Pure Appl Chem* 71(11):2117–2123. doi:[10.1351/pac199971112117](https://doi.org/10.1351/pac199971112117)
121. Walba DM, Dyer DJ, Sierra T, Cobben PL, Shao RF, Clark NA (1996) Ferroelectric liquid crystals for nonlinear optics: orientation of the disperse red 1 chromophore along the ferroelectric liquid crystal polar axis. *J Am Chem Soc* 118(5):1211–1212. doi:[10.1021/ja952387p](https://doi.org/10.1021/ja952387p)
122. Liu JY, Robinson MG, Johnson KM, Walba DM, Ros MB, Clark NA, Shao RF, Doroski D (1991) The measurement of 2nd-harmonic generation in novel ferroelectric liquid-crystal materials. *J Appl Phys* 70(7):3426–3430. doi:[10.1063/1.350330](https://doi.org/10.1063/1.350330)
123. Kapitza H, Zentel R, Twieg RJ, Nguyen C, Vallerien SU, Kremer F, Willson CG (1990) Ferroelectric liquid-crystalline polysiloxanes with high spontaneous polarization and possible applications in nonlinear optics. *Adv Mater* 2(11):539–543. doi:[10.1002/adma.19900021106](https://doi.org/10.1002/adma.19900021106)
124. Wischerhoff E, Zentel R, Redmond M, Mondainmonval O, Coles H (1994) Ferroelectric liquid-crystalline polysiloxanes designed for high 2nd-order nonlinear susceptibilities. *Macromol Chem Phys* 195(5):1593–1602. doi:[10.1002/macp.1994.021950511](https://doi.org/10.1002/macp.1994.021950511)
125. Kocot A, Wrzalik R, Vij JK, Brehmer M, Zentel R (1994) Dielectric and electrooptical studies of a ferroelectric copolysiloxane. *Phys Rev B* 50(22):16346–16356. doi:[10.1103/PhysRevB.50.16346](https://doi.org/10.1103/PhysRevB.50.16346)
126. Lehmann W, Leister N, Hartmann L, Geschke D, Kremer F, Stein P, Finkelmann H (1999) Piezoelectric and pyroelectric investigations on microtomed sections of single-crystalline

- ferroelectric liquid crystalline elastomers (SC-FLCE). *Mol Cryst Liq Cryst Sci Technol Sect A Mol Cryst Liq Cryst* 328:437–445. doi:[10.1080/10587259908026087](https://doi.org/10.1080/10587259908026087)
127. Leister N, Lehmann W, Weber U, Geschke D, Kremer F, Stein P, Finkelmann H (2000) Measurement of the pyroelectric response and of the thermal diffusivity of microtomed sections of 'single crystalline' ferroelectric liquid crystalline elastomers. *Liq Cryst* 27(2): 289–297. doi:[10.1080/026782900203119](https://doi.org/10.1080/026782900203119)
 128. Mauzac M, Nuyen HT, Tournilhac FG, Yablonsky SV (1995) Piezoelectric and pyroelectric properties of new polysiloxane smectic C* elastomers. *Chem Phys Lett* 240(5–6):461–466. doi:[10.1016/0009-2614\(95\)00574-n](https://doi.org/10.1016/0009-2614(95)00574-n)
 129. Ono H, Harato Y (1999) Characteristics of photothermal effects in guest-host liquid crystals by heat-conduction analysis. *J Opt Soc Am B Opt Phys* 16(12):2195–2201. doi:[10.1364/josab.16.002195](https://doi.org/10.1364/josab.16.002195)
 130. Shibaev VP, Kozlovsky MV, Beresnev LA, Blinov LM, Plate NA (1984) Thermotropic liquid crystalline polymers. 16. Chiral smectics C with spontaneous polarization. *Polym Bull* 12(4): 299–301. doi:[10.1007/bf00263142](https://doi.org/10.1007/bf00263142)
 131. Kostromin SG, Sinitzyn VV, Talroze RV, Shibaev VP, Plate NA (1982) Thermotropic liquid crystalline polymers. 12. Smectic C phase in liquid crystalline polyacrylates with CN-containing mesogenic groups. *Makromol Chem Rapid Commun* 3(11):809–814
 132. Vallerien SU, Zentel R, Kremer F, Kapitza H, Fischer EW (1989) Ferroelectric modes in combined side-group main chain liquid-crystalline polymers. *Makromol Chem Rapid Commun* 10(7):333–338
 133. Naciri J, Pfeiffer S, Shashidhar R (1991) Fast switching of ferroelectric side-chain liquid-crystalline polymer and copolymer. *Liq Cryst* 10(4):585–591. doi:[10.1080/02678299108036446](https://doi.org/10.1080/02678299108036446)
 134. Scherowsky G, Fichna U, Wolff D (1995) Ferroelectric liquid-crystalline polymers side-group derived from mesogenic vinyl ether monomers. *Liq Cryst* 19(5):621–627. doi:[10.1080/02678299508031076](https://doi.org/10.1080/02678299508031076)
 135. Cooray NF, Kakimoto M, Imai Y, Suzuki Y (1994) Novel fluorine-containing ferroelectric side-chain liquid-crystalline polysiloxanes showing bistable fast switching. *Macromolecules* 27(6):1592–1596. doi:[10.1021/ma00084a048](https://doi.org/10.1021/ma00084a048)
 136. Poths H, Schonfeld A, Zentel R, Kremer F, Siemensmeyer K (1992) Structure property relationships determining the spontaneous polarization in FLC-polymers. *Adv Mater* 4(5): 351–354. doi:[10.1002/adma.19920040507](https://doi.org/10.1002/adma.19920040507)
 137. Heinze P, Finkelmann H (2010) Shear deformation and ferroelectricity in chiral SmC* main-chain elastomers. *Macromolecules* 43(16):6655–6665. doi:[10.1021/ma1002084](https://doi.org/10.1021/ma1002084)
 138. Hiraoka K, Sagano W, Nose T, Finkelmann H (2005) Biaxial shape memory effect exhibited by monodomain chiral smectic C elastomers. *Macromolecules* 38(17):7352–7357. doi:[10.1021/ma050642c](https://doi.org/10.1021/ma050642c)
 139. Verduzco R, Luchetto P, Hong SH, Harden J, DiMasi E, Palffy-Muhoray P, Kilbey SM, Sprunt S, Gleeson JT, Jakli A (2010) Bent-core liquid crystal elastomers. *J Mater Chem* 20(39):8488–8495. doi:[10.1039/c0jm01920h](https://doi.org/10.1039/c0jm01920h)
 140. Spillmann CM, Ratna BR, Naciri J (2007) Anisotropic actuation in electroclinic liquid crystal elastomers. *Appl Phys Lett* 90(2):3. doi:[10.1063/1.2420780](https://doi.org/10.1063/1.2420780)
 141. Artal C, Ros MB, Serrano JL, Pereda N, Etxebarria J, Folcia CL, Ortega J (2001) SHG characterization of different polar materials obtained by in situ photopolymerization. *Macromolecules* 34(12):4244–4255. doi:[10.1021/ma001928e](https://doi.org/10.1021/ma001928e)
 142. Shashidhar R, Naciri J, Ratna BR (2000) Large electroclinic effect and associated properties of chiral smectic a liquid crystals. In: Prigogine I, Rice SA and Vij JK (eds) *Advances in chemical physics*, vol 113, John Wiley & Sons, Inc., Hoboken, NJ, USA. pp 51–76. doi:[10.1002/9780470141724.ch2](https://doi.org/10.1002/9780470141724.ch2)
 143. Kapernaum N, Walba DM, Korblova E, Zhu CH, Jones C, Shen YQ, Clark NA, Giesselmann F (2009) On the origin of the "giant" electroclinic effect in a "de Vries"-type ferroelectric liquid crystal material for chirality sensing applications. *ChemPhysChem* 10(6):890–892. doi:[10.1002/cphc.200900065](https://doi.org/10.1002/cphc.200900065)

144. Etxebarria J, Ros MB (2008) Bent-core liquid crystals in the route to functional materials. *J Mater Chem* 18(25):2919–2926. doi:[10.1039/b803507e](https://doi.org/10.1039/b803507e)
145. Ros MB, Serrano JL, de la Fuente MR, Folcia CL (2005) Banana-shaped liquid crystals: a new field to explore. *J Mater Chem* 15(48):5093–5098. doi:[10.1039/B504384k](https://doi.org/10.1039/B504384k)
146. Keith C, Reddy RA, Prehm M, Baumeister U, Kresse H, Chao JL, Hahn H, Lang H, Tschierske C (2007) Layer frustration, polar order and chirality in liquid crystalline phases of silyl-terminated achiral bent-core molecules. *Chemistry* 13(9):2556–2577. doi:[10.1002/chem.200600876](https://doi.org/10.1002/chem.200600876)
147. Reddy RA, Baumeister U, Keith C, Tschierske C (2007) Influence of the core structure on the development of polar order and superstructural chirality in liquid crystalline phases formed by silylated bent-core molecules: naphthalene derivatives. *J Mater Chem* 17(1):62–75. doi:[10.1039/b614089k](https://doi.org/10.1039/b614089k)
148. Weissflog W, Pelzl G, Kresse H, Baumeister U, Brand K, Schröder MW, Tamba MG, Findeisen-Tandel S, Kornek U, Stern S, Eremin A, Stannarius R, Svoboda J (2010) In search of a new design strategy for solid single-component organic ferroelectrics: polar crystalline phases formed by bent-core molecules. *J Mater Chem* 20(29):6057–6079. doi:[10.1039/c0jm00322k](https://doi.org/10.1039/c0jm00322k)
149. Keith C, Lehmann A, Baumeister U, Prehm M, Tschierske C (2010) Nematic phases of bent-core mesogens. *Soft Matter* 6(8):1704–1721. doi:[10.1039/b923262a](https://doi.org/10.1039/b923262a)
150. Tschierske C, Photinos DJ (2010) Biaxial nematic phases. *J Mater Chem* 20(21):4263–4294. doi:[10.1039/b924810b](https://doi.org/10.1039/b924810b)
151. Hult A, Sahlen F, Trollsas M, Lagerwall ST, Hermann D, Komitov L, Rudquist P, Stebler B (1996) A pyroelectric liquid crystal polymer (PLCP) for second-harmonic generation. *Liq Cryst* 20(1):23–28. doi:[10.1080/02678299608032022](https://doi.org/10.1080/02678299608032022)
152. Trollsas M, Orrenius C, Sahlen F, Gedde UW, Norin T, Hult A, Hermann D, Rudquist P, Komitov L, Lagerwall ST, Lindstrom J (1996) Preparation of a novel cross-linked polymer for second-order nonlinear optics. *J Am Chem Soc* 118(36):8542–8548. doi:[10.1021/ja961309e](https://doi.org/10.1021/ja961309e)
153. Trollsas M, Sahlen F, Gedde UW, Hult A, Hermann D, Rudquist P, Komitov L, Lagerwall ST, Stebler B, Lindstrom J, Rydlund O (1996) Novel thermally stable polymer materials for second-order nonlinear optics. *Macromolecules* 29(7):2590–2598. doi:[10.1021/ma9511154](https://doi.org/10.1021/ma9511154)
154. Davis FJ (1993) Liquid-crystalline elastomers. *J Mater Chem* 3(6):551–562. doi:[10.1039/JM9930300551](https://doi.org/10.1039/JM9930300551)
155. Gleim W, Finkelmann H (1989) Side chain liquid crystalline elastomers. In: McArdle CB (ed) *Side chain liquid crystalline polymers*. Blackie and Son, Glasgow
156. Finkelmann H (1991) Liquid-crystalline sidechain polymers. In: Ciferri A (ed) *Liquid crystallinity in polymers*. VCH, Weinheim
157. Hikmet RAM, Boots HMJ, Michielsen M (1995) Ferroelectric liquid-crystal gels - network stabilized ferroelectric displays. *Liq Cryst* 19(1):65–76. doi:[10.1080/02678299508036721](https://doi.org/10.1080/02678299508036721)
158. Hikmet RAM, Lub J (1996) Anisotropic networks and gels obtained by photopolymerisation in the liquid crystalline state: synthesis and applications. *Prog Polym Sci* 21(6):1165–1209. doi:[10.1016/S0079-6700\(96\)00017-2](https://doi.org/10.1016/S0079-6700(96)00017-2)
159. Tolksdorf C, Zentel R (2001) Reversible physical network stabilized ferroelectric liquid crystals. *Adv Mater* 13(17):1307–1310. doi:[10.1002/1521-4095\(200109\)13:17<1307::AID-ADMA1307>3.0.CO;2-7](https://doi.org/10.1002/1521-4095(200109)13:17<1307::AID-ADMA1307>3.0.CO;2-7)
160. Prigann J, Tolksdorf C, Skupin H, Zentel R, Kremer F (2002) FT-IR spectroscopic studies on reorientation of ferroelectric liquid crystals in a thermoreversible gel network. *Macromolecules* 35(10):4150–4154. doi:[10.1021/ma002065s](https://doi.org/10.1021/ma002065s)
161. Deindörfer P, Eremin A, Stannarius R, Davis R, Zentel R (2006) Gelation of smectic liquid crystal phases with photosensitive gel forming agents. *Soft Matter* 2(8):693–698. doi:[10.1039/b603562k](https://doi.org/10.1039/b603562k)
162. Meziane R, Brehmer M, Maschke U, Zentel R (2008) Gelling and the collective dynamics in ferroelectric liquid crystals. *Soft Matter* 4(6):1237–1241. doi:[10.1039/b800737c](https://doi.org/10.1039/b800737c)

163. Skarp K, Uto S, Myojin K, Moritake H, Ozaki M, Helgee B, Yoshino K (1995) Electrooptical and nonlinear-optical effects in free-surface films of polymeric ferroelectric liquid-crystals prepared by spin-coating method. *Jpn J Appl Phys Part 1-Regular Papers Short Notes & Review Papers* 34(9B):5433–5437. doi:[10.1143/JJAP.34.5433](https://doi.org/10.1143/JJAP.34.5433)
164. Gillberg G, Leube H, McKenzie L, Pruksarnukul L, Reeder L (1994) Self-assembled structures of azobenzene amphiphiles - a new photorecording medium. *J Appl Polym Sci* 53(5):687–699. doi:[10.1002/app.1994.070530519](https://doi.org/10.1002/app.1994.070530519)
165. Gebhard E, Zentel R (1998) Freestanding ferroelectric elastomer films. *Macromol Rapid Commun* 19(7):341–344. doi:[10.1002/\(SICI\)1521-3927\(19980701\)19:7<341::AID-MARC341>3.0.CO;2-S](https://doi.org/10.1002/(SICI)1521-3927(19980701)19:7<341::AID-MARC341>3.0.CO;2-S)
166. Benné I, Semmler K, Finkelmann H (1995) Mechanically induced 2nd-harmonic generation in SC* elastomers. *Macromolecules* 28(6):1854–1858
167. Benné I, Semmler K, Finkelmann H (1994) 2nd-harmonic generation on mechanically oriented S(C)*-elastomers. *Macromol Rapid Commun* 15(4):295–302
168. Papadopoulos P, Heinze P, Finkelmann H, Kremer F (2010) Electromechanical properties of smectic c* liquid crystal elastomers under shear. *Macromolecules* 43(16):6666–6670. doi:[10.1021/ma1005028](https://doi.org/10.1021/ma1005028)
169. Harden J, Chambers M, Verduzco R, Luchette P, Gleeson JT, Sprunt S, Jakli A (2010) Giant flexoelectricity in bent-core nematic liquid crystal elastomers. *Appl Phys Lett* 96(10):102907. doi:[10.1063/1.3358391](https://doi.org/10.1063/1.3358391)
170. Lehmann W, Skupin H, Tolksdorf C, Gebhard E, Zentel R, Krüger P, Lösche M, Kremer F (2001) Giant lateral electrostriction in ferroelectric liquid-crystalline elastomers. *Nature* 410(6827):447–450. doi:[10.1038/35068522](https://doi.org/10.1038/35068522)
171. Köhler R, Stannarius R, Tolksdorf C, Zentel R (2005) Electroclinic effect in free-standing smectic elastomer films. *Appl Phys A-Mater Sci Process* 80(2):381–388. doi:[10.1007/s00339-003-2267-5](https://doi.org/10.1007/s00339-003-2267-5)
172. Hiraoka K, Kobayasi M, Kazama R, Finkelmann H (2009) Electromechanics of monodomain chiral smectic c elastomer: mechanical response to electric stimulation. *Macromolecules* 42(15):5600–5604. doi:[10.1021/ma900761w](https://doi.org/10.1021/ma900761w)
173. Stannarius R, Köhler R, Dietrich U, Lösche M, Tolksdorf C, Zentel R (2002) Structure and elastic properties of smectic liquid crystalline elastomer films. *Phys Rev E* 65(4):11. doi:[04170710.1103/PhysRevE.65.041707](https://doi.org/10.1103/PhysRevE.65.041707)
174. Walba DM, Yang H, Shoemaker RK, Keller P, Shao RF, Coleman DA, Jones CD, Nakata M, Clark NA (2006) Main-chain chiral smectic polymers showing a large electroclinic effect in the SmA* phase. *Chem Mater* 18(19):4576–4584. doi:[10.1021/cm0606373](https://doi.org/10.1021/cm0606373)
175. Walba DM, Keller P, Shao RF, Clark NA, Hillmyer M, Grubbs RH (1996) Main-chain ferroelectric liquid crystal oligomers by acyclic diene metathesis polymerization. *J Am Chem Soc* 118(11):2740–2741. doi:[10.1021/ja953779z](https://doi.org/10.1021/ja953779z)
176. Keller P, Shao RF, Walba DM, Brunet M (1995) The first high polarization ferroelectric main-chain liquid-crystalline polymers. *Liq Cryst* 18(6):915–918. doi:[10.1080/02678299508036710](https://doi.org/10.1080/02678299508036710)
177. Brehmer M, Zentel R (1995) Ferroelectric liquid-crystalline elastomers with short switching times. *Macromol Rapid Commun* 16(9):659–662. doi:[10.1002/marc.1995.030160904](https://doi.org/10.1002/marc.1995.030160904)
178. Jakli A, Saupe A (1995) Mechanical vibrations of smectic cells under fast field reversal. *Mol Cryst Liq Cryst Sci Technol Sect A Mol Cryst Liq Cryst* 263:103–111. doi:[10.1080/10587259508033574](https://doi.org/10.1080/10587259508033574)
179. Jakli A, Saupe A (1996) Field-induced thickness change of ferroelectric liquid crystal films. *Phys Rev E* 53(6):R5580–R5583
180. Hiraoka K, Toyoda S, Hourai Y, Tokita M, Watanabe J (2010) Influence of DC electric field on soft mode of main-chain ferroelectric liquid-crystalline polyesters: polymeric effect on collective fluctuation. *Appl Phys Express* 3(1). doi:[10.1143/APEX.3.011701](https://doi.org/10.1143/APEX.3.011701)

181. Jakli A, Pintre IC, Serrano JL, Ros MB, de la Fuente MR (2009) Piezoelectric and electric-field-induced properties of a ferroelectric bent-core liquid crystal. *Adv Mater* 21(37): 3784–3788. doi:[10.1002/adma.200900131](https://doi.org/10.1002/adma.200900131)
182. Chambers M, Verduzco R, Gleeson JT, Sprunt S, Jakli A (2009) Calamitic liquid-crystalline elastomers swollen in bent-core liquid-crystal solvents. *Adv Mater* 21(16):1622–1626. doi:[10.1002/adma.200802739](https://doi.org/10.1002/adma.200802739)
183. Chambers M, Verduzco R, Gleeson JT, Sprunt S, Jakli A (2009) Flexoelectricity of a calamitic liquid crystal elastomer swollen with a bent-core liquid crystal. *J Mater Chem* 19(42):7909–7913. doi:[10.1039/b911652d](https://doi.org/10.1039/b911652d)
184. Kramer D, Brömmel F, Finkelmann H (2012) LC Elastomers – Synthesis and Mechanical Behavior. *Adv Polym Sci*. Springer, Heidelberg, Berlin (in print)
185. Urayama K (2011) Electro-Opto-Mechanical Effects in Swollen Nematic LC Elastomers. *Adv Polym Sci*. doi:[10.1007/12_2010_107](https://doi.org/10.1007/12_2010_107)
186. De Jeu WH, Ostrovskii BI (2011) Order and Disorder in Liquid-Crystalline Elastomers. *Adv Polym Sci*. doi:[10.1007/12_2010_105](https://doi.org/10.1007/12_2010_105)
187. Palfy-Muhoray P (2012) Liquid Crystal Elastomers and Light. *Adv Polym Sci*. doi:[10.1007/12_2011_165](https://doi.org/10.1007/12_2011_165)